

Asymptotic Spectral Efficiency of Multiuser Multisignature CDMA in Frequency-Selective Channels

Matthew J. M. Peacock, *Member, IEEE*, Iain B. Collings, *Senior Member, IEEE*, and Michael L. Honig, *Fellow, IEEE*

Abstract—This paper presents an asymptotic analysis of multisignature code-division multiple access (CDMA) in the presence of frequency-selective channels. We characterize the sum spectral efficiency and spectral efficiency regions for both the optimal and linear minimum mean-squared error (MMSE) multiuser receivers. Both independent and identically distributed (i.i.d.) signatures and isometric signatures, which are orthogonal at each transmitter, are considered. Our results are asymptotic as the number of signatures per user and processing gain both tend to infinity with fixed ratio. The spectral efficiency of the MMSE receiver is determined from the asymptotic output signal-to-interference-plus noise ratio (SINR). For isometric signatures, our results rely on approximating certain covariance matrices with unitarily invariant matrices that are asymptotically free. This approximation is shown to be very accurate through comparison with both simulation and an “incremental-signature” analysis, which can be used to compute asymptotic moments. Also, a novel proof of the convergence of the empirical spectral distribution of the signal correlation matrix is presented. From these results, we derive the optimal coding–spreading tradeoff, which maximizes the MMSE spectral efficiency, for the case of a single user with multiple i.i.d. signatures. Simulation studies demonstrate that the asymptotic results accurately predict the performance of finite-size systems of interest. The resulting expressions are used to highlight and infer properties of the multisignature CDMA system, including the benefit of orthogonal relative to i.i.d. signatures, and the tradeoff between spectral efficiency and the versatility of providing a variable data rate service through multiple signatures.

Index Terms—Capacity, code-division multiple access (CDMA), multiuser detection.

I. INTRODUCTION

BROADBAND wireless networks require transmission schemes which are resilient to both time- and frequency-selective fading, while supporting flexible per-user data

Manuscript received February 17, 2004; revised December 30, 2004. The work of M. J. M. Peacock was supported in part by the Australian CSIRO. The work of M. L. Honig was supported by the U.S. Army Research Office under Contract DAAD190310119 and by the National Science Foundation under Grant CCR-0310809. The material in this paper was presented in part at the IEEE International Symposium on Information Theory, Chicago, IL, June/July 2004 and at GLOBECOM’04, San Francisco, CA, December 2004.

M. J. M. Peacock is with the School of Electrical and Information Engineering, The University of Sydney, NSW 2006, Australia (e-mail: mpeac@ee.usyd.edu.au).

I. B. Collings was with the School of Electrical and Information Engineering, The University of Sydney, NSW 2006, Australia. He is now with CSIRO ITC Centre, Epping NSW 1710, Australia (e-mail: iain.collings@csiro.au).

M. L. Honig is with the Department of Electrical and Computer Engineering, Northwestern University, Evanston, IL 60208 USA (e-mail: mh@ece.northwestern.edu).

Communicated by M. Médard, Associate Editor for Communications.
Digital Object Identifier 10.1109/TIT.2005.864427

rates. Code-division multiple access (CDMA) with multiple signatures per user is well suited for this purpose [1]–[3]. Multisignature CDMA can be implemented in either conventional direct-sequence (DS) mode, or multicarrier (MC) mode [4]. An important advantage of these schemes is that they can operate with minimal coordination among users, since the number of signatures (and hence the data rate) can be chosen independently by the users. In contrast, orthogonal schemes such as orthogonal frequency-division multiple access (OFDMA) require the users to coordinate their transmitted spectra. As with OFDMA, both DS and MC CDMA can employ a cyclic prefix to remove the interference from previous symbols, and to diagonalize the channel matrix, and hence simplify receiver processing. Linear receivers, such as the matched filter, decorrelator, and linear minimum mean-squared error (MMSE) can be used either in the time or frequency domains.

We consider a multisignature CDMA system with a general channel model which only requires statistical knowledge of the channel eigenvalues. For example the model includes the up-link of a multiuser multisignature MC-CDMA system with frequency-selective fading channels, where each user spreads data bits across subcarriers using a set of frequency-domain signatures, as in [4], [5]. It also applies to multisignature versions of standard symbol-synchronous DS-CDMA systems with frequency-selective fading channels.

In this paper, we characterize the asymptotic spectral efficiency of multisignature CDMA. Asymptotic refers to the limit as both the number of signatures per user and spreading gain both tend to infinity with fixed ratio, which is called the *system load*. As in earlier work on the asymptotic spectral efficiency of DS-CDMA [6], [7], we consider both the MMSE and optimal receivers. We emphasize, however, that the asymptotic analysis presented here differs from prior large system analyses of DS-CDMA (e.g., [6]–[12]) in that we allow multiple signatures per user, and *fix* the number of users. By varying the system load across users, we are able to compute an associated spectral efficiency *region*, in addition to the sum spectral efficiency.

We consider two types of signature assignments, namely random independent and identically distributed (i.i.d.) signatures, and random isometric signatures in which the signatures assigned to a particular user are orthogonal but are independent of other users’ signatures. Note that with frequency-selective channels and multiple users, the orthogonality of isometric signatures is lost at the receiver. As such, it is not clear *a priori* whether isometric signatures have any advantage over i.i.d. signatures. (Note that in [13] it was observed that isometric

signatures do have advantages for a single user with multiple signatures.)

Related asymptotic analyses of DS-CDMA with i.i.d. signatures are presented in [12], which considers multisignature DS-CDMA with flat fading, and in [7], [10], [11], which consider single-signature DS-CDMA with flat and frequency-selective fading. In previous work, we derived the asymptotic signal-to-interference-plus-noise ratio (SINR) for CDMA with the MMSE receiver for a single-user with multiple i.i.d. signatures, and multiple users with an equal number of i.i.d. signatures per user [14]. A related asymptotic analysis of MC-CDMA has also been independently presented with i.i.d. signatures in [15], and with both i.i.d. and isometric signatures in [13], however the multiuser multisignature case has not been considered.

In this paper, we consider the general multiuser case, where there is no restriction on the allocation of signatures among users. We compute the asymptotic output SINR of the MMSE receiver with both i.i.d. and isometric signatures, which is then used to compute asymptotic spectral efficiency. (Note that the asymptotic SINR can also be used to evaluate both uncoded and coded bit error rates, as in [11], [14].) We also compare the results to the (optimal) asymptotic spectral efficiency of the CDMA channel. For isometric signatures, our results rely on approximating user covariance matrices with unitarily invariant matrices that are asymptotically free.¹ This approximation becomes exact for a large number of users, and is shown to be accurate for any number of users through comparisons with both simulation results and an “incremental-signature” analysis which evaluates the incremental change in the quantity of interest when a user adds a single signature. This method can be used to evaluate asymptotic moments, and to establish asymptotic convergence of performance measures.

The asymptotic expressions are functions of the system loads across users, noise power, received powers, and the fading properties of the channel (i.e., first-order distribution). In the case of a single user with multiple i.i.d. signatures and the MMSE receiver, we solve for the optimal load, or equivalently, the optimal spreading-coding tradeoff, which maximizes spectral efficiency. Although, strictly speaking, our results for isometric signatures are valid only for a large number of users, our numerical studies show that the analytical results accurately predict simulation results for all practical cases considered.

Our results allow us to illustrate the performance of multisignature CDMA with different parameters and operating conditions. For example, we examine the effect of allocating power to users in proportion to the number of assigned signatures, and quantify the expansion in spectral efficiency region relative to assigning each user equal power. Additional comparisons are made contrasting the performance with isometric and i.i.d. signatures, and with the optimal and MMSE receivers. We also compare the performance of CDMA with OFDMA, in which the users are orthogonal.

¹Free probability theory applies to sets of noncommuting random variables, which includes large random matrices as a canonical example [16], [17]. The notion of freeness in free probability theory is analogous to independence in classical probability theory. (A comprehensive treatment is given in [17].) Recent applications of free probability theory to communications problems have been presented in [10], [13], [18], [19]. See also the tutorial [20].

We now summarize our main results.

- The sum spectral efficiency *increases* with i.i.d. signatures, and *decreases* with isometric signatures, as the number of users increases, for a fixed total system load (summed over users) and $\frac{E_b}{N_0}$. This is true for both the MMSE and optimal receivers. Furthermore, the asymptotic sum spectral efficiency with isometric signatures is always higher than that with i.i.d. signatures. (Both spectral efficiencies converge to the same value as the number of users tends to infinity.) For example, with a total system load of three signatures per subchannel and $\frac{E_b}{N_0} = 10$ dB, as the number of users increases from one to infinity, the optimal sum spectral efficiency *increases* by about 25% with *i.i.d.* signatures and *decreases* by about the same percentage with *isometric* signatures. We therefore conclude that self-interference, caused by signatures which pass through the desired user’s channel, is more detrimental than interference from other users (i.e., signatures which pass through different channels) with i.i.d. signatures, but is less detrimental with isometric signatures. In both cases, more users means more channels, and hence more channel diversity. With i.i.d. signatures, this translates to a benefit for both the MMSE and optimal receivers. However, with isometric signatures adding users increases the correlation among signatures (on average) which compromises the diversity gain and leads to a net loss in performance.
- With an MMSE receiver, the user with the least number of signatures receives the highest (lowest) SINR with i.i.d. (isometric) signatures. This again implies that self-interference is worse (better) than other-user interference with i.i.d. (isometric) signatures.
- For a fixed number of equal power users, sum spectral efficiency is relatively insensitive to the load per user. However, for i.i.d. (isometric) signatures it is maximized (minimized) when each user has the same number of signatures, assuming the total load is fixed.
- In the infinite-user limit with a single signature per user, the spectral efficiency of CDMA with frequency-selective fading is the same as that of CDMA without fading (i.e., constant channel).

In Section II, we describe the CDMA system model. In Section III, we present the asymptotic spectral efficiency of CDMA with the optimal receiver, and in Section IV, we derive the asymptotic SINR for the MMSE receiver, along with the associated capacity. Numerical results, which illustrate the analysis, are presented in Section V, and conclusions are discussed in Section VI.

II. SYSTEM MODEL

We consider the uplink of a multisignature CDMA system with J synchronous users and frequency-selective channels. Let K denote the total number of signatures, and K_j denote the number of signatures assigned to user $j \in \mathcal{J}$, where $\mathcal{J} = \{1, \dots, J\}$. Let N denote the spreading gain, which is either the number of time-domain chips in DS-CDMA or the number of

subcarriers in MC-CDMA. We also refer to N as the number of transmit (and receive) dimensions. The ratio $\alpha = \sum_{j \in \mathcal{J}} K_j / N$ is the total *system load*, and $\alpha_j = K_j / N$ is the per-user load.

In matrix notation,² the sequence transmitted by user j during a CDMA symbol is of length N , and is given by $\mathbf{x}_j = \mathbf{S}_j \mathbf{b}_j$, where \mathbf{S}_j is the user's $N \times K_j$ signature matrix with the k th signature $\mathbf{s}_{j,k}$ in column k , and $\mathbf{b}_j = [b_{j,1}, b_{j,2}, \dots, b_{j,K_j}]^T$ is a vector of K_j data symbols. For convenience, we will absorb the different transmit power levels of the users into the channel model, and hence without loss of generality, we assume unit power, zero mean, i.i.d. data symbols with $\mathbf{E}[\mathbf{b}_j \mathbf{b}_j^\dagger] = \mathbf{I}_{K_j}$.

We consider both randomly assigned i.i.d. signatures and random orthogonal signatures for each user. In the i.i.d. case, the elements of $\sqrt{N} \mathbf{S}_j$ are i.i.d. circularly symmetric complex random variables, with zero mean, unit variance, and finite positive moments. The asymptotic performance results do not depend on the particular distribution of the elements. In the random orthogonal case, we assume that \mathbf{S}_j is obtained by extracting K_j columns from an $N \times N$ Haar-distributed³ unitary random matrix Θ_j , where $K_j \leq N$. We will assume that the matrices $\Theta_j, j = 1, \dots, J$, are independent. Note that [13] considers both i.i.d. and isometric signatures for MC-CDMA in frequency-selective fading with $J = 1$.

All users transmit their symbols synchronously, and any interference between successive CDMA symbols due to multipath is removed by the insertion of a cyclic prefix of length $G \geq M$. The received vector is

$$\mathbf{r} = \sum_{j \in \mathcal{J}} \mathbf{H}_j \mathbf{S}_j \mathbf{b}_j + \mathbf{n} \quad (1)$$

where \mathbf{H}_j is the channel matrix for user j , and \mathbf{n} is an $N \times 1$ vector of additive noise with i.i.d., circularly symmetric, complex Gaussian elements with zero mean and variance σ_n^2 . We also denote the average received power for each signature of the j th user as $p_j = \mathbf{E}[\text{Tr}[\mathbf{H}_j^\dagger \mathbf{H}_j]]$.

For DS-CDMA, \mathbf{H}_j is the standard circulant matrix constructed from the time-domain channel impulse response (CIR). For MC-CDMA, \mathbf{H}_j is diagonal where the diagonal contains the N -point discrete Fourier transform (DFT) of the CIR. The MC-CDMA channel \mathbf{H}_j^{MC} differs from the DS-CDMA channel \mathbf{H}_j^{DS} only in that \mathbf{H}_j^{MC} includes an additional IDFT/DFT operation, i.e.,

$$\mathbf{H}_j^{\text{MC}} = \mathbf{W}_F \mathbf{H}_j^{\text{DS}} \mathbf{W}_F^\dagger$$

where \mathbf{W}_F is the DFT matrix. Our analysis does not depend on the particular basis used, but rather depends only on the eigenvalues of $\mathbf{H}_j \mathbf{H}_j^\dagger$, which are clearly the same for both systems. Furthermore, if the channel order is finite, then the assumption of a cyclic prefix is unnecessary in either case as $N \rightarrow \infty$.

²**Notation:** All vectors are defined as column vectors and designated with bold lower case; all matrices are given in bold upper case; $(\cdot)^T$ denotes transpose; $(\cdot)^*$ denotes complex conjugate; $(\cdot)^\dagger$ denotes Hermitian (i.e., complex conjugate) transpose; $|\cdot|$ denotes matrix determinant; $\text{tr}[\cdot]$ denotes the matrix trace; $\text{Tr}[\cdot]$ denotes the normalized matrix trace $\text{tr}[\cdot]/N$; and, \mathbf{I}_N denotes the $N \times N$ identity matrix. Expectation and variance are denoted $\mathbf{E}[\cdot]$ and $\text{Var}[\cdot]$, respectively.

³An $N \times N$ random matrix Θ is Haar distributed if its probability distribution is invariant to left multiplication by any constant unitary matrix. If \mathbf{X} is an $N \times N$ random matrix with i.i.d. complex Gaussian centered unit variance entries, then the unitary matrix $\mathbf{X} \mathbf{X}^\dagger \mathbf{X}^{-1/2}$ is Haar distributed.

Therefore, our results apply equally to both DS-CDMA and MC-CDMA.

For the MMSE receiver, the estimate of the symbol carried on the k th signature for user j is given by

$$\hat{b}_{j,k} = \mathbf{s}_{j,k}^\dagger \mathbf{H}_j^\dagger \mathbf{R}^{-1} \mathbf{r} \quad (2)$$

where

$$\mathbf{R} = \sigma_n^2 \mathbf{I}_N + \sum_{u \in \mathcal{J}} \mathbf{R}_u \quad (3)$$

$$\mathbf{R}_u = \mathbf{H}_u \mathbf{S}_u \mathbf{S}_u^\dagger \mathbf{H}_u^\dagger. \quad (4)$$

The corresponding SINR is

$$\text{SINR}_{j,k} = \rho_{j,k}^N \quad (5)$$

where

$$\rho_{j,k}^N = \mathbf{s}_{j,k}^\dagger \mathbf{H}_j^\dagger \mathbf{R}_{d_{j,k}}^{-1} \mathbf{H}_j \mathbf{s}_{j,k} \quad (6)$$

and $\mathbf{R}_{d_{j,k}}$ denotes \mathbf{R} with the (j, k) th data stream removed, i.e.,

$$\mathbf{R}_{d_{j,k}} = \mathbf{R} - \mathbf{H}_j \mathbf{s}_{j,k} \mathbf{s}_{j,k}^\dagger \mathbf{H}_j^\dagger.$$

Throughout this paper, we consider the limit as N and $K_j \rightarrow \infty$ with $K_j/N \rightarrow \alpha_j$ for each $j \in \mathcal{J}$. We will denote this limit as “lim,” and evaluate the spectral efficiency in bits per chip. Note that each multisignature user can be considered as being equivalent to a fixed proportion of the users in single-signature CDMA systems (e.g., as considered in [9]).

When evaluating the limit as $N \rightarrow \infty$, we will assume that the bandwidth of the signal increases, as opposed to increasing the time duration of the symbol. In other words, as $N \rightarrow \infty$, the frequency diversity order increases in proportion with N . Furthermore, we will assume that the eigenvalues of $\mathbf{P}_j = \mathbf{H}_j \mathbf{H}_j^\dagger$ are uniformly bounded over N , i.e., $\sup_N \|\mathbf{P}_j\| < \infty$ for $j \in \mathcal{J}$, and that the empirical distribution of the N eigenvalues of \mathbf{P}_j for each $j \in \mathcal{J}$ converge in distribution almost surely to a deterministic distribution $F_{P_j}(\cdot)$, with mean p_j and compact support on the real nonnegative axis. With these assumptions, we will show that the spectral efficiency and MMSE SINR converge in the almost-sure sense as $N \rightarrow \infty$.

An example of a specific channel model which satisfies the preceding assumptions is a wideband frequency-selective fading channel with a finite-length impulse response, where the coefficients are modeled as zero-mean, complex-valued, circularly symmetric Gaussian random variables (i.e., Rayleigh fading). Here we use the term “wideband” to indicate that there are many coherence bands, so that a normalized histogram of the squared absolute value of the frequency domain channel gains is well approximated by an exponential probability density function (pdf). Technically, we must truncate the exponential distribution, in order to meet the requirement of compact support, however, the truncation value can be arbitrarily large. It can be verified that the associated truncation error vanishes as the truncation value tends to infinity.

III. SPECTRAL EFFICIENCY REGION

The *spectral efficiency* for user j , C_j , is defined as the maximum number of bits per chip summed over the user's signatures that can be reliably transmitted [6]. Since the bandwidth of a CDMA system is roughly equivalent to the reciprocal of the chip duration, the total spectral efficiency (summed over users) can

be viewed as the maximum bits per second per hertz (bits/s/Hz) supported by the system.

In this section, we derive the (optimal) asymptotic spectral efficiency region of the multiuser multisignature CDMA model. We start by considering the capacity region of the Gaussian multiple-access channel (GMAC) [21]. We then consider each boundary of the region, and express the boundaries in terms of Stieltjes transforms. Unfortunately, for isometric signatures, these transforms cannot be computed,⁴ however, we will make approximations to the transforms using free probability [17].

In what follows, we assume that the transmitter has no knowledge of the channel, hence, the information rate $R_{j,k}$, which is carried on signature k for user j , is independent of k . That is, for a particular user, the rate per signature does not vary across signatures, although the total rate R_j can vary with user j . This corresponds to coding the information sequence at rate R_j , and then spreading the coded symbols evenly across the user's signatures. The spectral efficiency for user j , and the sum spectral efficiency are therefore, respectively, given by

$$C_j = \frac{K_j}{N} R_j = \alpha_j R_j \quad (7)$$

$$C = \sum_{j \in \mathcal{J}} C_j. \quad (8)$$

The capacity region of the GMAC was derived in [21]. Since multisignature CDMA is a form of the GMAC channel with a specific mixing matrix, the corresponding capacity region is

$$\mathcal{S} = \bigcap_{\mathcal{I} \subseteq \mathcal{J}} \left\{ C_1, \dots, C_J : 0 \leq \sum_{i \in \mathcal{I}} C_i \leq C_{\mathcal{I}}^N(\sigma_n^2), \right. \\ \left. C_j = 0 \text{ for } j \notin \mathcal{I} \right\} \quad (9)$$

where

$$C_{\mathcal{I}}^N(\sigma_n^2) = \frac{1}{N} \log \left| \mathbf{I}_{K^{\mathcal{I}}} + \sigma_n^{-2} \mathbf{S}_{\mathcal{I}}^{\dagger} \mathbf{S}_{\mathcal{I}} \right| \quad (10)$$

$$K^{\mathcal{I}} = \sum_{i \in \mathcal{I}} K_i \quad (11)$$

$$\mathbf{S}_{\mathcal{I}} = [\mathbf{H}_{\mathcal{I}_1} \mathbf{S}_{\mathcal{I}_1} \quad \cdots \quad \mathbf{H}_{\mathcal{I}_{|\mathcal{I}|}} \mathbf{S}_{\mathcal{I}_{|\mathcal{I}|}}] \quad (12)$$

and \mathcal{I}_i denotes the i th element of the set \mathcal{I} , which is a subset of \mathcal{J} .

Note that the boundaries of the spectral efficiency region in (9), i.e., the values of $C_{\mathcal{I}}^N(\sigma_n^2)$, are random, since they depend on the particular realizations of \mathbf{H}_j and $\mathbf{S}_j, j \in \mathcal{J}$. We now proceed to obtain an asymptotic limit for each of the conditions in (9). Note that

$$C_{\mathcal{I}}^N(\sigma_n^2) = \frac{1}{N} \sum_{k=1}^{K^{\mathcal{I}}} \log(1 + \sigma_n^{-2} \lambda_k) \quad (13)$$

where λ_k is the k th eigenvalue of $\mathbf{S}_{\mathcal{I}}^{\dagger} \mathbf{S}_{\mathcal{I}}$ and $\mathcal{I} \subseteq \mathcal{J}$. Since the eigenvalues of $\mathbf{S}_{\mathcal{I}}^{\dagger} \mathbf{S}_{\mathcal{I}}$ and the nonzero eigenvalues of

$$\tilde{\mathbf{R}}_{\mathcal{I}} \triangleq \mathbf{S}_{\mathcal{I}} \mathbf{S}_{\mathcal{I}}^{\dagger} = \sum_{j \in \mathcal{I}} \mathbf{R}_j \quad (14)$$

⁴A more general case of this problem is solved using a novel approach in [22, Theorem 1].

are identical (where \mathbf{R}_j is defined in (4)), we can replace $\mathbf{S}_{\mathcal{I}}^{\dagger} \mathbf{S}_{\mathcal{I}}$ by $\tilde{\mathbf{R}}_{\mathcal{I}}$ in (10) and sum to N in (13), to obtain

$$C_{\mathcal{I}}^N(\sigma_n^2) = \frac{1}{N} \sum_{k=1}^N \log(1 + \sigma_n^{-2} \lambda_k) \quad (15)$$

$$= \int \log(1 + \sigma_n^{-2} \lambda) dF_{\tilde{\mathbf{R}}_{\mathcal{I}}}^N(\lambda) \quad (16)$$

where $F_{\tilde{\mathbf{R}}_{\mathcal{I}}}^N : \mathbb{R} \mapsto \mathbb{R}$ is the *empirical eigenvalue distribution* (e.e.d.) of the random matrix $\tilde{\mathbf{R}}_{\mathcal{I}}$, i.e.,

$$F_{\tilde{\mathbf{R}}_{\mathcal{I}}}^N(\lambda) = \frac{1}{N} \cdot |\{\lambda_i : \lambda_i \leq \lambda\}|.$$

In order to determine the asymptotic limit of (16), we

- i) determine the convergence of the (random) e.e.d. of $\tilde{\mathbf{R}}_{\mathcal{I}}$ to a (deterministic) *asymptotic eigenvalue distribution* (a.e.d.);
- ii) express the limit of (16) in terms of the Stieltjes transform of the a.e.d. of $\tilde{\mathbf{R}}_{\mathcal{I}}$; and
- iii) determine the Stieltjes transform of the a.e.d. of $\tilde{\mathbf{R}}_{\mathcal{I}}$.

In order to address item i) above, first note that all terms in the expansion of the k th moment of \mathbf{R} (and $\tilde{\mathbf{R}}_{\mathcal{I}}$) have the form considered in the following theorem.

Theorem 1: The family of $N \times N$ random matrices

$$\mathcal{S}_J^I = \{\mathbf{R}_1, \dots, \mathbf{R}_I, \mathbf{P}_1, \dots, \mathbf{P}_J, \sigma_n^2 \mathbf{I}_N\}, \quad 0 \leq I \leq J < \infty$$

has an almost-sure limit distribution. That is, $\kappa_{\underline{m}, N} \xrightarrow{\text{a.s.}} \kappa_{\underline{m}}$ as $(N, K_j) \rightarrow \infty, K_j/N \rightarrow \alpha_j > 0, j = 1 \dots J$, for all $\underline{m} \in \mathcal{M}(I + J + 1)$, where

- $\mathcal{M}(M)$ denotes the set of all finite-length sequences of positive integers from the set $\{1, \dots, M\}, M \in \mathbb{Z}^+$;
- $\kappa_{\underline{m}, N}$ is the empirical moment given by

$$\kappa_{\underline{m}, N} = \frac{1}{N} \text{tr} \left[\prod_{i=1}^{|\underline{m}|} \mathbf{X}_{\underline{m}(i)} \right]; \quad (17)$$

- \mathbf{X}_k is the k th element of \mathcal{S}_J^I ;
- $\kappa_{\underline{m}}$ is a deterministic polynomial in $\alpha_j, j = 1, \dots, I$, where the degree of α_j is equal to

$$d_{\underline{m}, j} = |\{i | \underline{m}(i) \leq I, \underline{m}(i) = j, i = 1, \dots, |\underline{m}|\}| \quad (18)$$

and the coefficients of the polynomial are completely determined by σ_n^2 and finite moments of $\mathbf{P}_j, j \in \mathcal{J}$.

Proof: See Appendix II. \square

Theorem 1 establishes the convergence of the k th moment of $\mathbf{R}, k > 0$, for both i.i.d. and isometric signatures, which in turn establishes the almost-sure convergence in distribution of the e.e.d., since the spectral norm of \mathbf{R} is bounded.

With a trivial relabeling of the indices of $\mathbf{R}_j, j \in \mathcal{J}$, the above argument also holds for $\mathbf{R}_{\mathcal{I}}$ in place of \mathbf{R} . Moreover, as $\log(1 + \sigma_n^{-2} \lambda)$ is bounded and continuous on the support of the a.e.d. of $\tilde{\mathbf{R}}_{\mathcal{I}}$, from [32, Theorem 4.4.1], we conclude that $|C_{\mathcal{I}}^N(\sigma_n^2) - C_{\mathcal{I}}(-\sigma_n^2)| \xrightarrow{\text{a.s.}} 0$, where

$$C_{\mathcal{I}}(z) = \int \log(1 - z^{-1} \lambda) dF_{\tilde{\mathbf{R}}_{\mathcal{I}}}(\lambda) \quad (19)$$

and $F_{\tilde{\mathbf{R}}_{\mathcal{I}}} : \mathbb{R} \mapsto \mathbb{R}$ denotes the a.e.d. of $\tilde{\mathbf{R}}_{\mathcal{I}}$. The argument z is introduced in (19) in order to express $C_{\mathcal{I}}(z)$ in terms of the

Stieltjes transform⁵ of $F_{\tilde{\mathbf{R}}_{\mathcal{I}}}$, using the following method from [18]. Differentiating (19) with respect to z gives

$$\frac{dC_{\mathcal{I}}(z)}{dz} = -G_{\tilde{\mathbf{R}}_{\mathcal{I}}}(z) - z^{-1}. \quad (20)$$

Using the boundary condition $\lim_{z \rightarrow -\infty} C_{\mathcal{I}}(z) = 0$ (i.e., the spectral efficiency goes to zero as the noise level increases to infinity), we have

$$C_{\mathcal{I}}(-\sigma_n^2) = - \int_{-\infty}^{-\sigma_n^2} \left(G_{\tilde{\mathbf{R}}_{\mathcal{I}}}(z) + z^{-1} \right) dz \quad (21)$$

where $G_{\tilde{\mathbf{R}}_{\mathcal{I}}}$ is the Stieltjes transform of $F_{\tilde{\mathbf{R}}_{\mathcal{I}}}$. This completes step ii) described above.

Step iii) requires determining $G_{\tilde{\mathbf{R}}_{\mathcal{I}}}(z)$ for both i.i.d. and isometric signatures, as considered separately in the following subsections.

A. i.i.d. Signatures

To determine $G_{\tilde{\mathbf{R}}_{\mathcal{I}}}(z)$ for i.i.d. signatures, first define

$$\gamma_{\mathcal{I}}^N(z) = \text{Tr}[(\tilde{\mathbf{R}}_{\mathcal{I}} - z\mathbf{I}_N)^{-1}] \quad (22)$$

$$\rho_{j,\mathcal{I}}^N(z) = \text{Tr}[\mathbf{P}_j(\tilde{\mathbf{R}}_{\mathcal{I}} - z\mathbf{I}_N)^{-1}] \quad (23)$$

and note that $\gamma_{\mathcal{I}}^N(z)$ is the Stieltjes transform of the e.e.d. of $\tilde{\mathbf{R}}_{\mathcal{I}}$. Also, note that we use the notation $\rho_{j,\mathcal{I}}^N(z)$ for the term in (23), since it is shown in Section IV to be directly related to $\rho_{j,k}^N$ in (6).

An application of [24, Theorem 16.3]⁶ gives that as $(N, K_j) \rightarrow \infty$ with $K_j/N \rightarrow \alpha_j$, $|\gamma_{\mathcal{I}}^N(z) - G_{\tilde{\mathbf{R}}_{\mathcal{I}}}(z)| \xrightarrow{\text{a.s.}} 0$ and $|\rho_{j,\mathcal{I}}^N(z) - \rho_{j,\mathcal{I}}| \xrightarrow{\text{a.s.}} 0$, where $G_{\tilde{\mathbf{R}}_{\mathcal{I}}}(z)$ and $\rho_{j,\mathcal{I}}$ are the solutions to the following set of $|\mathcal{I}| + 1$ equations:

$$G_{\tilde{\mathbf{R}}_{\mathcal{I}}}(z) = -z^{-1} \left(1 - \alpha + \sum_{j \in \mathcal{I}} \frac{\alpha_j}{1 + \rho_{j,\mathcal{I}}} \right) \quad (24)$$

$$\rho_{j,\mathcal{I}} = \mathbf{E} \left[H_j \left(-z + \sum_{i \in \mathcal{I}} \frac{\alpha_i H_i}{1 + \rho_{i,\mathcal{I}}} \right)^{-1} \right], \quad j = 1 \in \mathcal{I}. \quad (25)$$

where the expectation in (25) is with respect to $\{H_i\}_{i \in \mathcal{I}}$, and H_i is a scalar random variable according to the a.e.d. of $\mathbf{H}_i \mathbf{H}_i^\dagger$. In addition, for $z \in \mathbb{C}^+$, a unique solution $G_{\tilde{\mathbf{R}}_{\mathcal{I}}}(z) \in \mathbb{C}^+$, $\rho_{j,\mathcal{I}} \in \mathbb{C}^+$, $j \in \mathcal{I}$ to (24)–(25) exists.

B. Isometric Signatures

For isometric \mathbf{S} , determining $G_{\tilde{\mathbf{R}}_{\mathcal{I}}}(z)$ is not straightforward, since the matrices \mathbf{R}_j , $j = 1, \dots, J$, are not asymptotically free.⁷ If they were, then the a.e.d. of the sum could be computed

⁵The Stieltjes (or Cauchy) transform of the distribution of a random variable $X \in \mathbb{R}^*$ is $\mathbf{E}[\frac{1}{X-z}]$, where $z \in \mathbb{C}^+$ is the transform variable, and

$$\mathbb{C}^+ = \{x | x \in \mathbb{C}, \text{Im}(x) > 0\}.$$

⁶The authors thank P. Loubaton for bringing this reference to our attention.

⁷We show in Appendix I that $\lim \text{Tr}[\mathbf{R}_1 \mathbf{R}_2 \mathbf{R}_1 \mathbf{R}_2]$ is not the same as the corresponding limit obtained by assuming that \mathbf{R}_1 and \mathbf{R}_2 are asymptotically free.

by using the R-transform.⁸ Nevertheless, we will see that there is negligible error (for all cases considered) associated with approximating the component matrices in \mathbf{R} by asymptotically free matrices. We therefore proceed by defining

$$\tilde{\mathbf{R}}_{\mathcal{I}} = \sum_{j \in \mathcal{I}} \tilde{\mathbf{R}}_j \quad (26)$$

where $\tilde{\mathbf{R}}_j = \mathbf{U}_j \mathbf{R}_j \mathbf{U}_j^\dagger$, and $\{\mathbf{U}_j\}_{j \in \mathcal{I}}$ is a set of independent random unitary matrices. Note that \mathbf{R}_j and $\tilde{\mathbf{R}}_j$ have the same eigenvalues, and the matrices $\tilde{\mathbf{R}}_j$, $j = 1, \dots, J$ are asymptotically free since they are unitarily invariant, and have an almost-sure limit distribution due to a straightforward extension of Theorem 1, and thus satisfy [17, Theorem 4.3.5]. We will approximate $G_{\mathbf{R}_j}(z)$ with $G_{\tilde{\mathbf{R}}_j}(z)$. The accuracy of this approximation is discussed in Section V-A and in Appendix I. Note that it becomes exact for large J . Namely, as J increases, the elements of \mathbf{R} become Gaussian, in which case the a.e.d. of $\tilde{\mathbf{R}}_{\mathcal{I}}$ and $\tilde{\mathbf{R}}_{\mathcal{I}}$ is the fixed point of the R-transform.

Using this approach, we will show that Stieltjes transform $G_{\tilde{\mathbf{R}}_{\mathcal{I}}}(z)$, satisfies the following $|\mathcal{I}| + 1$ equations:

$$G_{\tilde{\mathbf{R}}_{\mathcal{I}}}(z) = \frac{|\mathcal{I}| - 1}{z - \sum_{j \in \mathcal{I}} z_j} \quad (27)$$

$$G_{\tilde{\mathbf{R}}_{\mathcal{I}}}(z) = G_{\mathbf{P}_j} \left(z_j \left(1 + \frac{1 - \alpha_j}{z_j G_{\tilde{\mathbf{R}}_{\mathcal{I}}}(z)} \right)^{-1} \right) - \frac{1 - \alpha_j}{z_j}, \quad \text{for } j \in \mathcal{I}, \alpha_j \leq 1 \quad (28)$$

where $G_{\mathbf{P}_j}(z)$ denotes the Stieltjes transform of the a.e.d. of \mathbf{P}_j .

To see this, first note that $\tilde{\mathbf{R}}_j$ has the same eigenvalues as $\mathbf{S}_j \mathbf{S}_j^\dagger \mathbf{P}_j$. Now, note that $\mathbf{S}_j \mathbf{S}_j^\dagger$ can be written as $\Theta_j \mathbf{E}_j \mathbf{E}_j^\dagger \Theta_j^\dagger$, where the $N \times N$ matrix $\mathbf{E}_j = \text{diag}([1, \dots, 1, 0, \dots, 0])$ with $\text{tr}[\mathbf{E}_j] = K_j < N$. From [17, Proposition 4.3.9], the family $\{\mathbf{P}_j, \mathbf{S}_j \mathbf{S}_j^\dagger\}$ is almost-surely asymptotically free, and the Stieltjes transform $G_{\tilde{\mathbf{R}}_j}(z)$ can be computed by applying the S-transform [25]. The S-transform computation is summarized by the following identity. Namely, the Stieltjes transform of the distribution of the product of two noncommutative free random variables, $c = ab$, is the solution to the following three equations (written in compact form) in the three unknowns $G_c(z)$, z_a , and z_b :

$$G_c(z) = \frac{1}{z(z z_a z_b - 1)} = \frac{1}{z z_a} G_a(z_a^{-1}) = \frac{1}{z z_b} G_b(z_b^{-1}) \quad (29)$$

where $G_a(z)$ and $G_b(z)$ denotes the Stieltjes transform of the distributions of a and b , respectively.

Applying this to $\tilde{\mathbf{R}}_j$ gives

$$G_{\tilde{\mathbf{R}}_j}(z) = \frac{1}{z(z z_1 z_2 - 1)} = \frac{1}{z z_1} G_{\mathbf{P}_j}(z_1^{-1}) = \frac{1}{z} \left(\frac{\alpha_j}{z_2 - 1} - (1 - \alpha_j) \right) \quad (30)$$

⁸The R- and S-transforms allow the computation of the distribution of sums and products, respectively, of noncommutative free random variables. See, e.g., [17], [20].

Now, (30) can be rewritten as the fixed-point equation

$$G_{\underline{\mathbf{R}}_j}(z) = G_{\mathbf{P}_j} \left(z \left(1 + \frac{1 - \alpha_j}{z G_{\underline{\mathbf{R}}_j}(z)} \right)^{-1} \right) - \frac{1 - \alpha_j}{z}. \quad (31)$$

Applying the R-transform to (26) with (31) gives the result.

Note that in the particular case of frequency-selective Rayleigh fading discussed in Section II (for which the a.e.d. of \mathbf{P}_j is an exponential distribution with mean p_j)

$$G_{\mathbf{P}_j}(z) = -\frac{1}{z} f \left(-\frac{p_j}{z} \right) \quad (32)$$

$$f(x) = x^{-1} \exp(x^{-1}) \text{Ei}(x^{-1}) \quad (33)$$

$$\text{Ei}(x) = \int_1^\infty e^{-xt} t^{-1} dt \quad (34)$$

and hence, (28) simplifies to

$$G_{\underline{\mathbf{R}}_j}(z) = -\frac{1}{z_j} f \left(\frac{p_j(\alpha_j - 1)}{z_j^2 G_{\underline{\mathbf{R}}_j}(z)} - \frac{p_j}{z_j} \right), \quad \text{for } j \in \mathcal{I}, \alpha_j \leq 1. \quad (35)$$

In summary, (21) is evaluated using (24)–(25) or (27)–(28) in order to determine the boundaries of the asymptotic spectral efficiency region.

IV. MMSE RECEIVER SPECTRAL EFFICIENCY

In this section, we consider the performance of a system with an MMSE receiver. Asymptotically, the interference-plus-noise at the output of the MMSE receiver is Gaussian [26], hence, the asymptotic capacity per signature for user j with a single-signature decoder is $\log(1 + \rho_j)$ [27] where ρ_j is the asymptotic output SINR of the MMSE receiver for the j th user, defined below. The asymptotic total (sum) capacity with single-signature decoders is therefore

$$C_{\text{MMSE}}^\infty = \sum_{j \in \mathcal{J}} \alpha_j \log(1 + \rho_j). \quad (36)$$

We now require the asymptotic MMSE SINRs $\rho_j, j \in \mathcal{J}$.

With i.i.d. signatures, [10, Lemma 1] and [23, Lemma 2.6] applied to (6) give

$$\max_{k \leq K_j} |\rho_{j,k}^N - \rho_j^N| \xrightarrow{\text{a.s.}} 0 \quad (37)$$

as $(N, K_j) \rightarrow \infty$ with $K_j/N \rightarrow \alpha_j$ for $j \in \mathcal{J}$, where

$$\rho_j^N = \text{Tr}[\mathbf{P}_j \mathbf{R}^{-1}] \quad (38)$$

which corresponds to $\rho_{j,\mathcal{I}}^N(z)$ with $z = -\sigma_n^2$ and $\mathcal{I} = \mathcal{J}$, as defined in (23). Therefore, solving (24)–(25) at $z \rightarrow -\sigma_n^2$ gives the asymptotic SINR.

We note that an alternate approach to deriving the SINR in this i.i.d. case is presented in [33]. There a set of simultaneous equations is derived using an incremental signature method (see Appendix I) in terms of the derivatives $\partial G_{\mathbf{R}}(z)/\partial \alpha_j$ and the moments $\text{Tr}\{\mathbf{R}^{-1}\}$ and $\text{Tr}\{\mathbf{R}^{-2}\}$. However, in [33], the moments were evaluated using the free approximation we use here for isometric signatures.

To compute the asymptotic MMSE SINR with isometric signatures, we use a generalization of the approach presented in

[13] for $J = 1$. As in the previous subsection, we will employ an approximation in order to use the S-transform. The mean-squared error (MSE) for user j is given by $1 - \eta_{j,k}$, where

$$\eta_{j,k}^N = \mathbf{s}_{j,k}^\dagger \mathbf{H}_j^\dagger \mathbf{R}^{-1} \mathbf{H}_j \mathbf{s}_{j,k} \quad (39)$$

and the corresponding SINR is $\rho_{j,k}^N = \frac{\eta_{j,k}^N}{1 - \eta_{j,k}^N}$. From Lemma 1 in Appendix I and [23, Lemma 2.6], we have that

$$\max_{k \leq K_j} |\alpha_j \eta_{j,k}^N - \text{Tr}[\mathbf{R}^{-1} \mathbf{R}_j]| \xrightarrow{\text{a.s.}} 0 \quad (40)$$

in the limit considered, and moreover

$$\begin{aligned} & \text{Tr}[\mathbf{R}_j(\mathbf{R}_j + \mathbf{R}_{j-})^{-1}] \\ &= \text{Tr} \left[\mathbf{R}_j \left(\mathbf{R}_{j-}^{-1} - \mathbf{R}_{j-}^{-1} (\mathbf{I} + \mathbf{R}_j \mathbf{R}_{j-}^{-1})^{-1} \mathbf{R}_j \mathbf{R}_{j-}^{-1} \right) \right] \end{aligned} \quad (41)$$

$$= \mathbf{E} \left[X_j - \frac{X_j^2}{1 + X_j} \right] = \mathbf{E} \left[\frac{X_j}{1 + X_j} \right] \quad (42)$$

where the second equality is the matrix inversion lemma, and X_j is a random variable with distribution according to the e.e.d. of $\mathbf{X}_j = \mathbf{R}_j \mathbf{R}_{j-}^{-1}$. Let $\Upsilon_{\mathbf{X}_j}(z) = -z^{-1} G_{\mathbf{X}_j}(z^{-1}) - 1$, where $G_{\mathbf{X}_j}(z)$ is the Stieltjes transform of a.e.d. of \mathbf{X}_j , which exists due to Theorem 1. We then have from (40) that

$$\max_{k \leq K_j} |\alpha_j \eta_{j,k} + \Upsilon_{\mathbf{X}_j}(-1)| \xrightarrow{\text{a.s.}} 0 \quad (43)$$

We again approximate $G_{\mathbf{X}_j}(z)$ by $G_{\underline{\mathbf{X}}_j}(z)$, where $\underline{\mathbf{X}}_j = \mathbf{R}_j \underline{\mathbf{R}}_{j-}^{-1}$ and

$$\underline{\mathbf{R}}_{j-} = \sigma_n^2 \mathbf{I}_N + \sum_{u=1, u \neq j}^J \underline{\mathbf{R}}_u.$$

Since \mathbf{R}_j and $\underline{\mathbf{R}}_{j-}$ are asymptotically free (from [17, Theorem 4.3.5]), we can compute the Stieltjes transform of a.e.d. of $\underline{\mathbf{X}}_j$, namely, $G_{\underline{\mathbf{X}}_j}$, via the S-transform. Equivalently, we may transform and apply the S-transform identity given in (29), to obtain

$$\Upsilon_{\underline{\mathbf{X}}_j}(z) = \frac{z_1 z_2}{z - z_1 z_2} = \Upsilon_{\mathbf{R}_j}(z_1) = \Upsilon_{\underline{\mathbf{R}}_{j-}^{-1}}(z_2) \quad (44)$$

where $\Upsilon_{\mathbf{R}_j}(z)$ can be determined from $G_{\mathbf{R}_j}(z)$, given in (31). Also,

$$\Upsilon_{\underline{\mathbf{R}}_{j-}^{-1}}(z) = \mathbf{E} \left[\frac{\tilde{\lambda}^{-1} z}{1 - \tilde{\lambda}^{-1} z} \right] = \mathbf{E} \left[\frac{z}{\tilde{\lambda} - z} \right] = z G_{\underline{\mathbf{R}}_{j-}}(z) \quad (45)$$

where $\tilde{\lambda}$ is a real-valued random variable with distribution given by the a.e.d. of $\underline{\mathbf{R}}_{j-}$, and $G_{\underline{\mathbf{R}}_{j-}}(z)$ is given by (27)–(28), where $\mathcal{I} = \mathcal{J}/\{j\}$.

Summarizing the preceding derivations, we have

$$\Upsilon_{\underline{\mathbf{X}}_j}(z) = \frac{z_1 z_2}{z - z_1 z_2} \quad (46)$$

$$\Upsilon_{\underline{\mathbf{X}}_j}(z) = -\frac{1}{z_1} G_{\mathbf{P}_j} \left(\frac{\Upsilon_{\underline{\mathbf{X}}_j}(z) + 1}{z_1 (\Upsilon_{\underline{\mathbf{X}}_j}(z) + \alpha_j)} \right) - \alpha_j \quad (47)$$

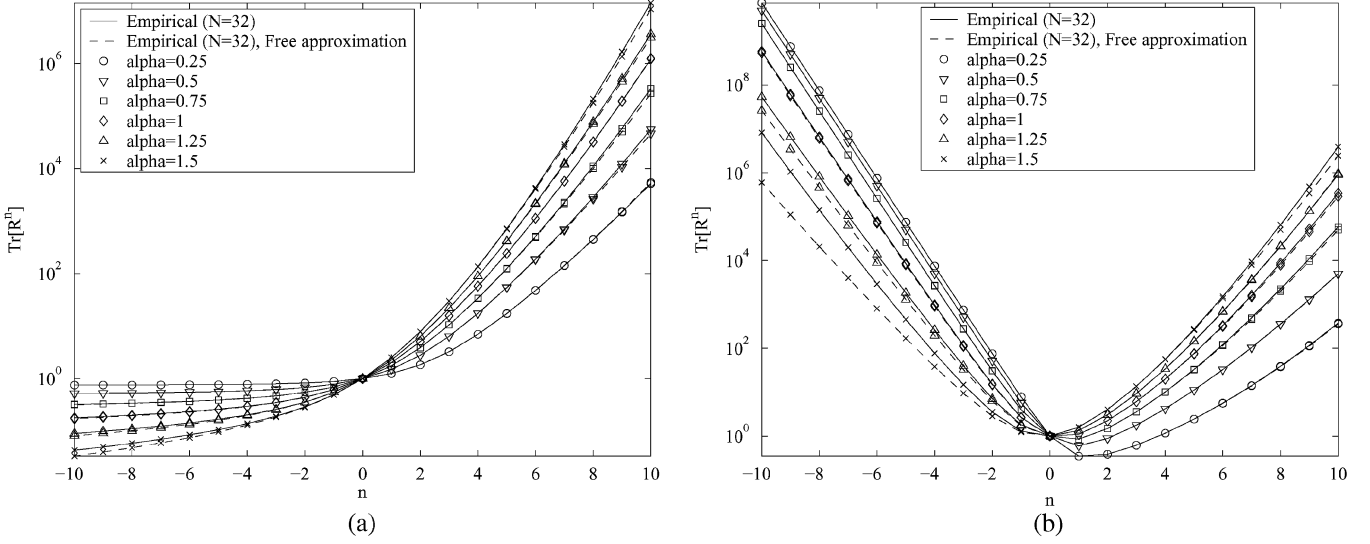


Fig. 1. Empirical ($N = 32$) positive and negative moments of \mathbf{R} and $\underline{\mathbf{R}}$ (labeled Free approximation) for $J = 2$ equal-power users with isometric signatures. (a) 0 dB per-signature SNR, (b) 10 dB per-signature SNR.

$$\Upsilon_{\underline{\mathbf{X}}_j}(z) = \frac{(J-2)z_2}{z_2 - \sigma_n^2 - \sum_{u \in \mathcal{J}/\{j\}} x_u} \quad (48)$$

$$\Upsilon_{\underline{\mathbf{X}}_j}(z) = z_2 G_{\mathbf{P}_u} \left(x_u \left(1 + \frac{z_2(1-\alpha_u)}{x_u \Upsilon_{\underline{\mathbf{X}}_j}(z)} \right)^{-1} \right) - \frac{z_2(1-\alpha_u)}{x_u}, \quad u \in \mathcal{J}/\{j\}. \quad (49)$$

These relations specify $\Upsilon_{\underline{\mathbf{X}}_j}(z)$ as a system of $J+2$ nonlinear equations in $J+2$ unknowns. The unknown variables are $\{\Upsilon_{\underline{\mathbf{X}}_j}(z), z_1, z_2, \mathbf{x}_j\}$, where $\mathbf{x}_j = \{x_u | u \in \mathcal{J}/\{j\}\}$. The asymptotic MSE can therefore be computed from (43) and (46)–(49).

V. NUMERICAL RESULTS

A. Accuracy of Free Approximation for Isometric Signatures

1) *Comparison of Moments of \mathbf{R} and $\underline{\mathbf{R}}$* : The results for isometric signatures in this paper are based on approximating the a.e.d. of \mathbf{R} by the a.e.d. of $\underline{\mathbf{R}}$. In this section, we discuss the accuracy of this approximation by comparing the moments of \mathbf{R} and $\underline{\mathbf{R}}$. Identical asymptotic moments would imply that the a.e.d.'s are the same.

Fig. 1 shows plots of the moments $\text{Tr}[\mathbf{R}^n]$ and $\text{Tr}[\underline{\mathbf{R}}^n]$ versus n for $J = 2$, $N = 32$, $\alpha_j = \alpha/J$, and per-signature received SNRs p_j/σ_n^2 as 0 and 10 dB with isometric signatures. These plots are obtained by averaging over 2000 realizations of the respective matrices. They show that the approximation is very accurate over a wide range of parameters (SNRs and system load α). The approximation becomes less accurate as α increases beyond $\alpha = 1$, in particular, for the large negative moments, and for high per-signature SNR. Similar plots for $J > 2$ show that the differences between the moments of \mathbf{R} and $\underline{\mathbf{R}}$ diminish further. As discussed in Section III, as J increases, these differences must tend to zero since the a.e.d.'s of \mathbf{R} and $\underline{\mathbf{R}}$ converge to the same distribution.

The asymptotic positive moments of \mathbf{R} and $\underline{\mathbf{R}}$ can be computed exactly via an incremental-signature technique. In Appendix I, we show that the first three asymptotic moments are identical, and that the differences in the higher moments are polynomials in the per-user system loads $\{\alpha_j\}$ and average received power per signature p_j , $j = 1, \dots, J$, and the noise power per receive dimension σ_n^2 . This implies that the approximation is very accurate for $\alpha < 1$ and low SNR, as observed in Fig. 1.

B. Comparison of $G_{\tilde{\mathbf{R}}_T}(z)$ and $G_{\underline{\mathbf{R}}_T}(z)$

The Stieltjes transform $G_{\tilde{\mathbf{R}}}(z)$ is used in (21) to compute the asymptotic optimal spectral efficiency, and is also used to compute the asymptotic MMSE SINR. Fig. 2 compares $G_{\tilde{\mathbf{R}}_T}(z)$ computed empirically for $N = 16$ (since asymptotic results are not available) with $G_{\underline{\mathbf{R}}_T}(z)$ for real, negative z , and two users with isometric signatures, equal powers and loads. Note that the approximation is most accurate for $\alpha < 1$.

1) *Comparison of Empirical and Approximate Asymptotic Sum Spectral Efficiency*: Fig. 3 compares empirical values of C_T^N with (approximate) asymptotic values of C_T for $\mathcal{I} = \{1, 2\}$ as a function of α over a range of per-signature SNRs (0–20 dB in 2-dB steps) for two users with isometric signatures, equal power and loads. Empirical curves represent averages over 2000 realizations of (13) with $N = 32$. The approximation is nearly exact for all points shown. The small but visible differences between the empirical and approximate curves shown in Fig. 2 for small values of z therefore introduce negligible error when computing sum spectral efficiency.

2) *Comparison of Empirical and Approximate Asymptotic SINR for Two Users*: Fig. 4 shows empirical ($N = 32$) and asymptotic values of output MMSE SINR ρ_j^N and ρ_j versus α for two equal-power users with $\alpha_2 = 3\alpha_1$. Curves are shown for per-signature received SNR ranging from zero to 20 dB, in steps of 2 dB, along with infinite SNR.

These results again show that the asymptotic approximation made for isometric signatures is very accurate, especially for

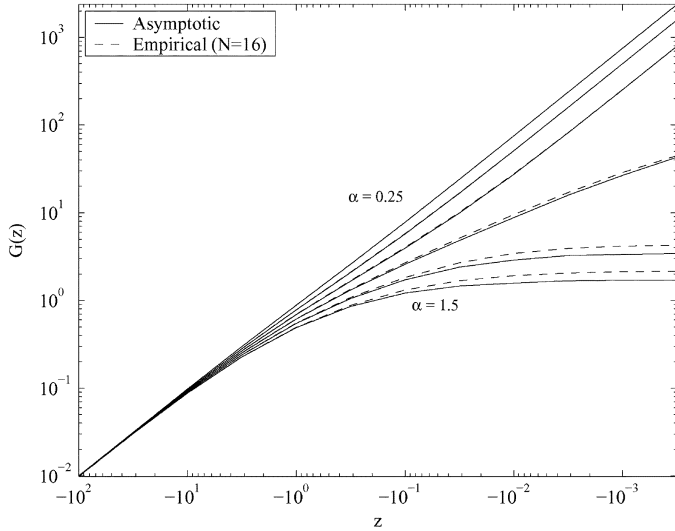


Fig. 2. Empirical ($N = 16$) values of $G_{\mathbf{R}_I}(z)$ and asymptotic values of $G_{\mathbf{R}_I}(z)$ versus real, negative z for two users with isometric signatures, equal power and loads. Curves shown are for $I = \{1, 2\}$ and $\alpha = 0.25$ to 1.5 in steps of 0.25.

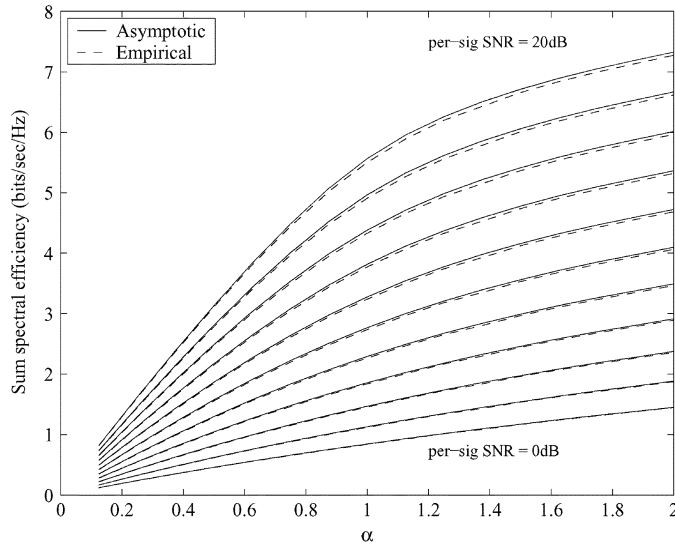


Fig. 3. Empirical and (approximate) asymptotic values of sum spectral efficiency versus α , over a range of per-signature SNRs (in 2-dB steps), for two users with isometric signatures, equal power and loads.

$\alpha < 1$. The small differences between the empirical and approximate asymptotic curves in Fig. 2 therefore contributes negligible error.

Note that for i.i.d. signatures, the asymptotic SINR is higher for the transmitter with the least number of signatures, even though the received power per signature is the same for all signatures in the system. For isometric signatures, the reverse is true.

3) *Comparison of Empirical and Approximate Asymptotic SINR for Four Users:* Fig. 5 shows empirical ($N = 128$) and asymptotic values of output SINR ρ_j^∞ versus α , for $J = 4$ equal-power users with $\alpha_1 = \alpha/2, \alpha_2 = \alpha/4, \alpha_3 = 3\alpha/16$, and $\alpha_4 = \alpha/16$. Again, these curves show close alignment between the asymptotic and empirical values. As in Fig. 4, we observe that the output SINR for a particular transmitter decreases

(increases) as the load increases for i.i.d. (isometric) signatures, even though the received power per signature is the same for all signatures in the system. This indicates that for i.i.d. signatures, self-interference, caused by signatures which pass through the desired user's channel, is slightly worse than interference from other users, i.e., signatures which pass through different channels. For isometric signatures the reverse is true.

C. Asymptotic Spectral Efficiency

The preceding numerical comparisons show that the asymptotic results give very accurate predictions of finite-system performance. Hence, in what follows we only show asymptotic results, and omit comparisons with empirical results for finite-size systems.

1) *Two-User Asymptotic Spectral Efficiency Regions:* Consider two users, each with equal variance per Rayleigh sub-channel $p_1 = p_2$. Each user allocates equal power across his own signatures, that is, at the receiver $\text{SNR}_{j,k} = p_j \mathbf{s}_{j,k}^\dagger \mathbf{s}_{j,k} / \sigma_n^2$ does not depend on k . We shall consider two power assignment schemes. In the first, the power per user is proportional to the user's system load (i.e., equal-power per signature). This is motivated by current CDMA systems in which the rate per user is varied by varying the number of assigned signatures. We will refer to this scheme as *proportional* power allocation. In the second scheme, we assume that each user is assigned *equal* power. In both cases, the sum total power over the two users is equal, and the two schemes are identical when $\alpha_1 = \alpha_2$.

Fig. 6(a) shows three asymptotic optimal spectral efficiency regions with proportional power allocation corresponding to different values of α_1 with $\alpha_1 + \alpha_2 = 1$ and per-signature receive SNR = 8 dB. Regions are shown for both i.i.d. and isometric signatures, based on numerical integration of $G_{\mathbf{R}_T}(z)$ and $G_{\mathbf{R}_I}(z)$ for $I = \{1, 2\}$, respectively, according to (21). Note also that, for isometric signatures, the horizontal and vertical boundaries are exact asymptotic values (calculated using the exact single-user expressions), whereas the boundaries on sum spectral efficiency are approximate. Also shown is the corresponding region with MMSE receivers and i.i.d. signatures, assuming single-signature decoders. Fig. 6(b) shows the union of asymptotic spectral efficiency regions over all α_1 such that $\alpha_1 + \alpha_2 = 1$, where all other parameters are the same as in Fig. 6(a).

As expected, Fig. 6(a) shows that the spectral efficiency for a particular user increases with the number of assigned signatures, or load. With i.i.d. signatures, the boundary of the spectral efficiency region is concave, and the sum capacity $C_1 + C_2$ is maximized with $\alpha_1 = \alpha_2 = 0.5$, whereas with isometric signatures the boundary is convex, and the sum capacity is *minimized* at $\alpha_1 = \alpha_2 = 0.5$; the maximum is at either $\alpha_1 = 0$ or 1. Still, the minimum sum spectral efficiency with isometric signatures is greater than the maximum spectral efficiency with i.i.d. signatures. This again implies that with i.i.d. signatures self-interference corresponding to a signature from the same user is more harmful than interference corresponding to a signature from another user. In contrast, with isometric signatures self-interference is *less* harmful than other-user interference.

Also shown in Fig. 6(b) are the regions corresponding to OFDMA with additive white Gaussian noise (AWGN) and

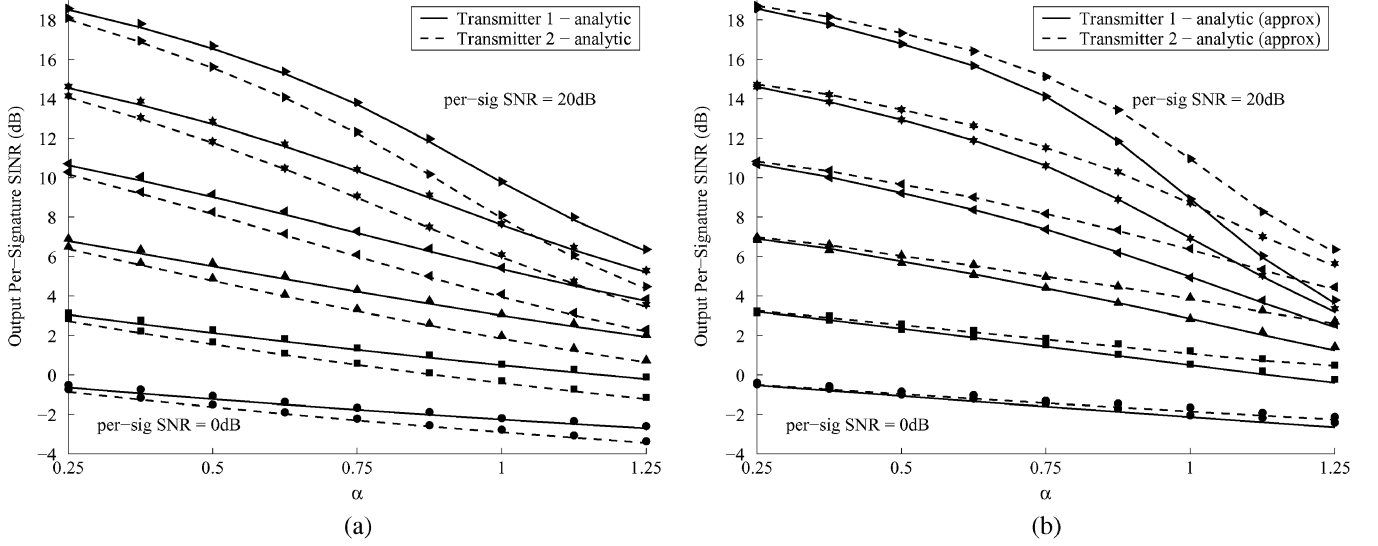


Fig. 4. Empirical ($N = 32$) and asymptotic values of output SINR ρ_j^N and ρ_j versus α for two equal-power transmitters with $\alpha_2 = 3\alpha_1$. Curves are shown for per-signature received SNR from zero to 20 dB, in steps of 4 dB. (a) i.i.d. signatures, (b) isometric signatures.

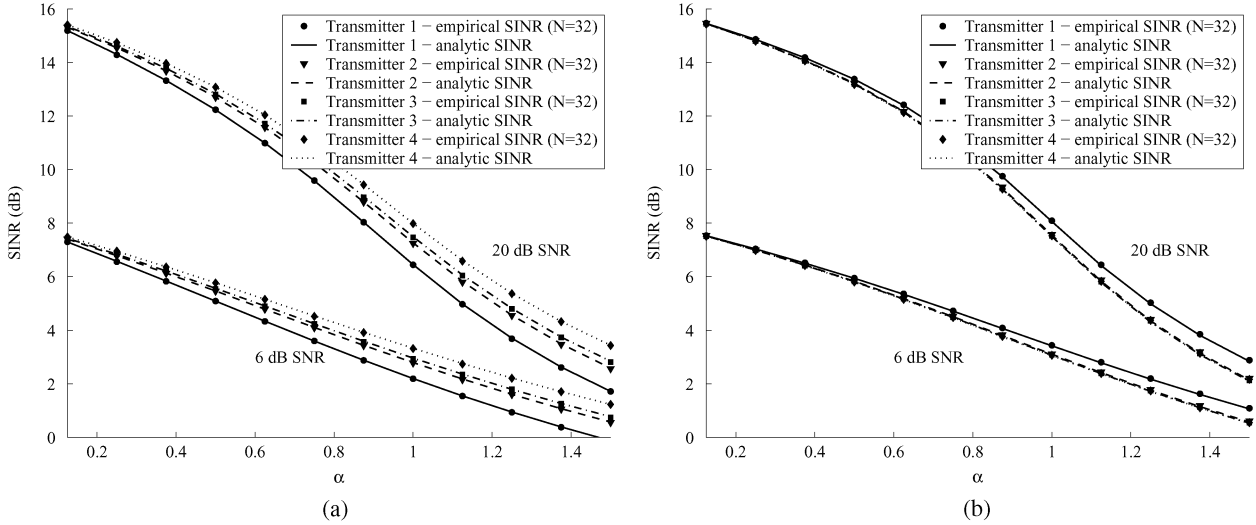


Fig. 5. Empirical ($N = 128$) and asymptotic values of output SINR ρ_j^N and ρ_j versus α for four equal-power transmitters with $\alpha_1 = \alpha/2, \alpha_2 = \alpha/4, \alpha_3 = 3\alpha/16, \alpha_4 = \alpha/16$. Curves are shown for per-signature received SNR at 6 and 20 dB. (a) i.i.d. signatures, (b) isometric signatures.

Rayleigh-fading channels. In OFDMA, the users occupy nonoverlapping sets of subchannels, and hence there is no multiuser interference. In that case, the system load α_j designates the fraction of total bandwidth allocated to user j . For the case $\alpha = 1$ considered, the curves are given by

$$C_{\text{AWGN}}^{\text{OFDMA}}(\sigma_n^2) = \log_2(1 + \sigma_n^{-2}) \quad (50)$$

$$C_{\text{Fading}}^{\text{OFDMA}}(\sigma_n^2) = \int_0^\infty \log_2(1 + \sigma_n^{-2}x) e^{-x} dx. \quad (51)$$

The figure shows that the capacity region of fully loaded OFDMA ($\alpha = 1$), which is an orthogonal multiple-access scheme, is larger than that of CDMA. This is also true for CDMA sum capacity with one signature per user [6]. Of course, OFDMA is limited to $\alpha \leq 1$, requires more coordination among users, and is also more susceptible to interference from other cells and cochannel systems. As α increases beyond one, the spectral efficiency region of CDMA becomes larger than that of OFDMA in Rayleigh-fading channels, as indicated later in Fig. 9.

Fig. 6(b) shows that the CDMA curve with isometric signatures meets the OFDMA fading curve at the axes. In other words, a single CDMA user with $\alpha = 1$ and isometric signatures has the same spectral efficiency as OFDMA, even though the CDMA signatures are not orthogonal at the receiver. This is because the CDMA spectral efficiency is $\frac{1}{N} \sum_{n=1}^N \log(1 + \sigma_n^{-2} \lambda_n)$ where $\{\lambda_n\}$ are the eigenvalues of $\mathbf{H}^\dagger \mathbf{H}$ for OFDMA, and $\mathbf{S}^\dagger \mathbf{H}^\dagger \mathbf{H} \mathbf{S}$ for CDMA. With isometric signatures, these eigenvalues are the same in both cases.

Fig. 7(a) and (b) shows the union of asymptotic spectral efficiency regions over α_1 for two users with proportional and equal-power allocation, respectively. Regions are shown for total loads $\alpha_1 + \alpha_2 = \alpha = 0.5, 0.75$ and 1, per-signature received SNR = 8 dB, and with both i.i.d. and isometric signatures. In both cases, the region expands as α increases. These graphs show that proportional power allocation gives a larger spectral efficiency region than allocating equal power per user. Note that with only one active user, corresponding to the intersection of the boundary with each axis, proportional power

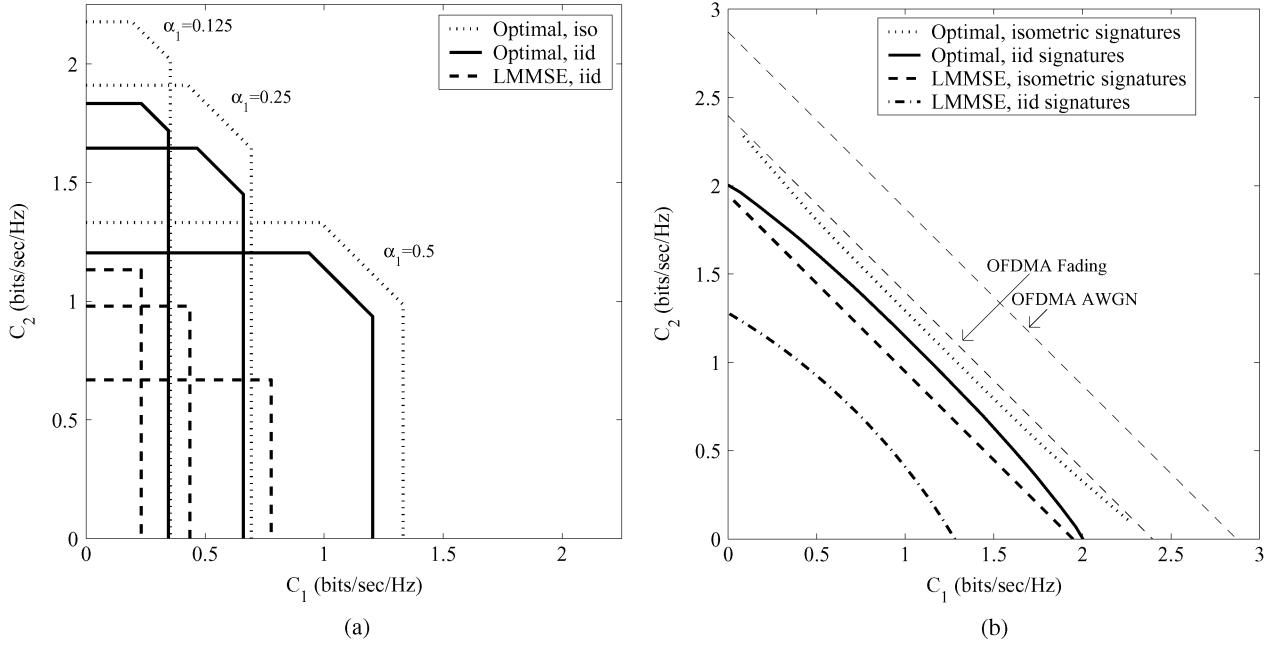


Fig. 6. Asymptotic optimal spectral efficiency regions with i.i.d. and isometric signatures. Also shown is the corresponding region with the MMSE receiver, i.i.d. signatures, and single-signature decoding. All curves are for two users, proportional power allocation, and SNR = 8 dB. (a) Three regions with $\alpha_1 + \alpha_2 = 1$. (b) Union of all regions with $\alpha_1 + \alpha_2 = 1$.

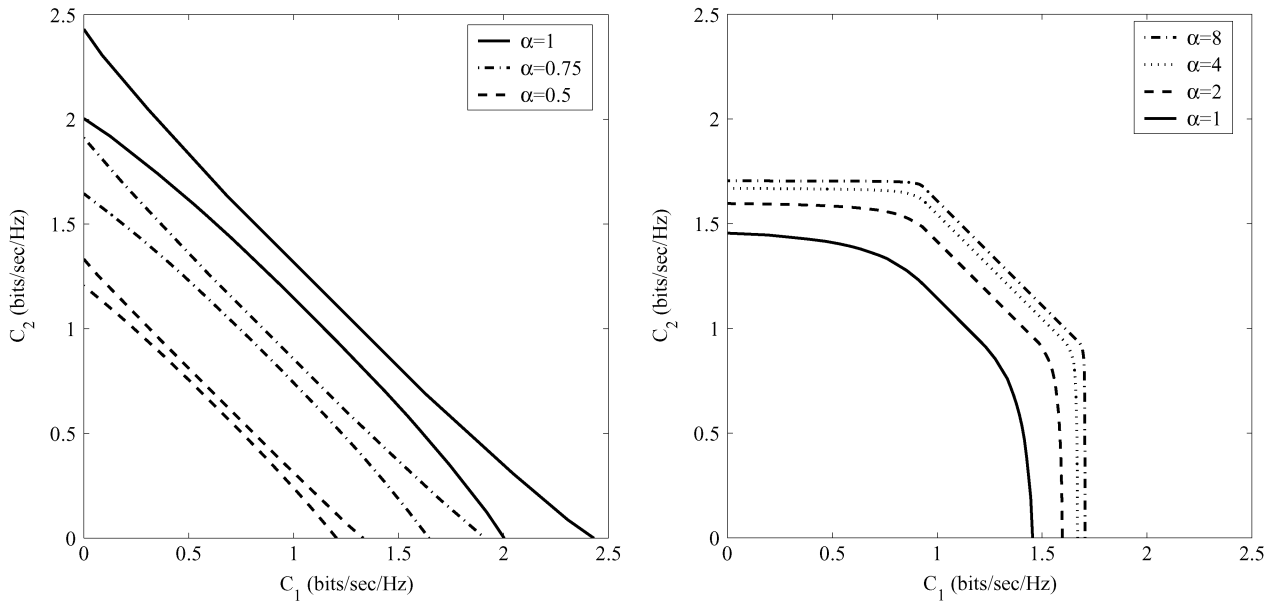


Fig. 7. Union of asymptotic spectral efficiency regions for two users with $\alpha_1 + \alpha_2 = \alpha$. (a) Curves correspond to proportional power allocation with i.i.d. and isometric signatures. For each α , the region corresponding to isometric signatures is larger than the region corresponding to i.i.d. signatures. The received per-signature SNR = 8 dB. (b) Curves correspond to equal power per user with i.i.d. signatures. The per-signature SNR satisfies $J\alpha_j p_j / \sigma_n^2 = 8$ dB, so that the total transmit power is the same as for proportional power allocation with $\alpha = 1$.

assignment allocates twice as much power to the active user as equal-power assignment.

2) *Spectral Efficiency Versus $\frac{E_b}{N_0}$ and System Load*: Fig. 8 shows asymptotic sum spectral efficiency versus $\frac{E_b}{N_0}$ for OFDMA and CDMA with i.i.d. and isometric signatures for $J = 1, 2, 4$, and K users, and proportional power allocation. In each case $\alpha_j = 1/J$, so that $\alpha = 1$. Note that

$$\frac{E_b}{N_0} = \frac{\text{SNR}}{R} = \frac{\alpha \text{SNR}}{C}.$$

(The isometric $J = 1$ and OFDMA curves coincide.)

Fig. 8(a) and (b) shows that as J increases, the spectral efficiency increases with i.i.d. signatures, but decreases with isometric signatures. Note that the $J = K$ curve is common to both figures, so that the asymptotic spectral efficiency with isometric signatures is always greater than that for i.i.d. signatures, and the difference goes to zero as J increases.

Fig. 9 shows asymptotic sum spectral efficiency versus total system load α for OFDMA and CDMA with i.i.d. and isometric signatures for $J = 1, 2, 4$, and K users, and proportional power allocation with $\frac{E_b}{N_0} = 10$ dB. In each case $\alpha_j = \alpha/J$. Also

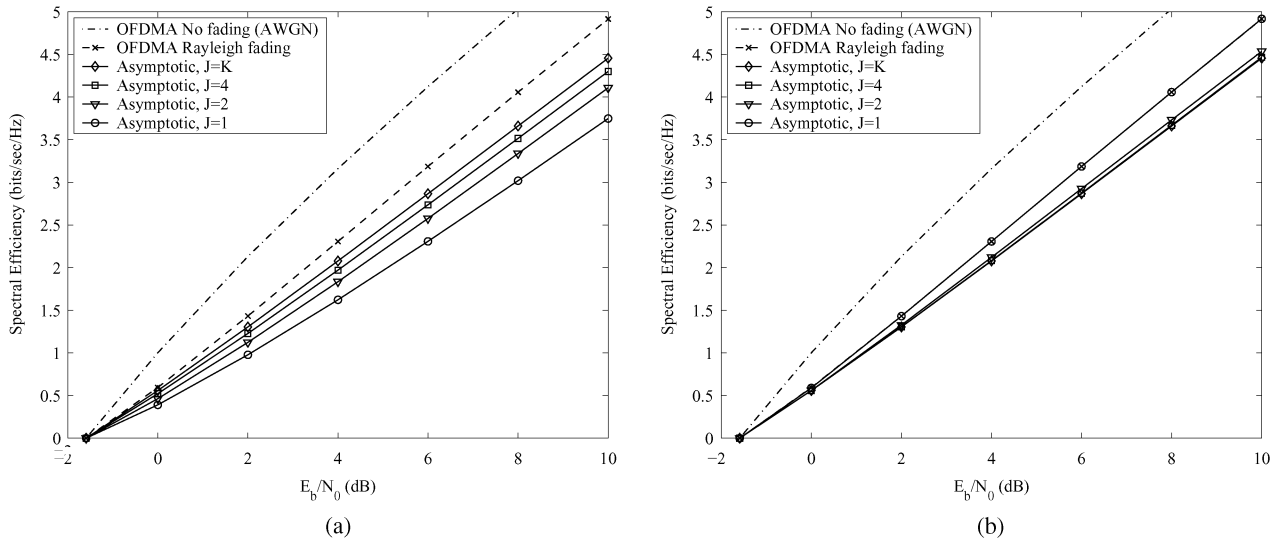


Fig. 8. Sum spectral efficiency vs. $\frac{E_b}{N_0}$ for OFDMA and CDMA for $J = 1, 2, 4$ and K users, and proportional power allocation. In each case $\alpha_j = 1/J$ so that $\alpha = 1$. (a) i.i.d. signatures, (b) isometric signatures.

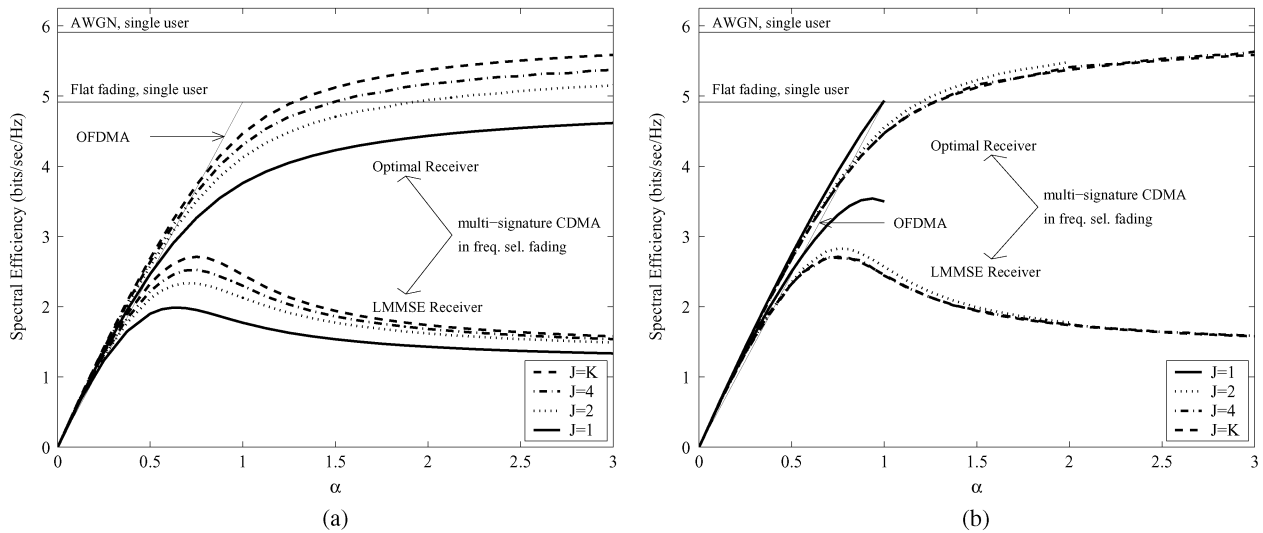


Fig. 9. Sum spectral efficiency versus α for OFDMA and CDMA for $J = 1, 2, 4$, and K users, and proportional power allocation with $\frac{E_b}{N_0} = 10$ dB. In each case $\alpha_j = \alpha/J$. (a) i.i.d. signatures, (b) isometric signatures.

shown are the single-user spectral efficiencies with AWGN and flat fading, given by (50) and (51), respectively. Fig. 9(a), corresponding to i.i.d. signatures, shows curves for both the optimal receiver (from (21) and (24)–(25)) and the MMSE receiver (from (36) and (24)–(25)). As observed in [6] for the case of single-signature CDMA, the spectral efficiency of CDMA with an optimal receiver increases with α , whereas the spectral efficiency for the MMSE receiver reaches a maximum when the system load is less than one.

Fig. 9(a) shows that as $\alpha \rightarrow \infty$, the optimal spectral efficiency with $J = K$ (single signature per user) appears to approach the AWGN single-user spectral efficiency, and the single-user, multisignature spectral efficiency with i.i.d. signatures appears to approach the flat-fading single-user spectral efficiency. We also observe that the spectral efficiency of the MMSE receiver with i.i.d. signatures increases with J for fixed

α . This is due to the fact that self-interference is worse than other-user interference.

In the isometric signature case, presented in Fig. 8, curves are shown for both the optimal and MMSE receivers. Of course, in this case we must have $\alpha < J$. As in Fig. 8, the $J = K$ curve is the same for i.i.d. and isometric signatures. Again for any finite number of users, the spectral efficiency with isometric signatures is always greater than that with i.i.d. signatures.

For $J = 1$ and $\alpha = 1$, MC-CDMA with isometric signatures has the same spectral efficiency as OFDMA, as discussed in relation to Fig. 8(b). However, for $\alpha < 1$, the spectral efficiency is greater than that of OFDMA. This is due to the higher degree of frequency diversity obtained with MC-CDMA, because it spreads over all subcarriers. Also note that the MC-CDMA spectral efficiency decreases slightly as J increases, even though there is greater diversity with larger J . This is due to

the fact that the assigned signatures are not orthogonal among users. The minimum spectral efficiency with $J = K$ (i.e., a single signature per user) is greater than the spectral efficiency with i.i.d. signatures (for any J).

D. Discussion

The preceding numerical results indicate the effect of splitting a total number of signatures (i.e., system load) and power between two users. In general, the preceding analysis can be used to optimize the allocation of signatures and powers among many users to meet specific system objectives. For example, if each user has a target information rate, then we can determine a set of assigned powers and system loads, which can achieve these rates. An objective in that case might be to minimize the total power summed over the users. The set of powers and loads, which minimize the total power, appears to be difficult to determine analytically, but can be computed via a gradient search. For both the optimal and MMSE receivers, the total load α can also be considered a design parameter. For the optimal receiver, both the sum spectral efficiency and the receiver complexity increase with α . For the MMSE receiver, α can be selected to optimize the coding–spreading tradeoff, as previously discussed.

VI. CONCLUSION

We have analyzed the spectral efficiency of multiuser multisingature CDMA over frequency-selective fading channels. Both the optimal and MMSE receivers have been considered with i.i.d. and isometric random signatures. Our results are asymptotic as the number of signatures per user and processing gain tend to infinity with fixed ratio (system load), and account for variations in system load and transmitted power across users. By optimizing the system loads across users, we can compute a maximum achievable spectral efficiency region. The analysis has been used to illustrate the dependence of the spectral efficiency region on power and signature allocation across users, and the spectral efficiency of the optimal and MMSE receivers as a function of the code rate.

Our numerical results indicate that with i.i.d. signatures, self-interference from signatures which pass through the same channel as the desired signature, is worse than other-user interference, i.e., from signatures which pass through a different channel. Namely, we have observed that for the MMSE receiver, a user with a smaller system load experiences a higher output SINR. Also, for both the MMSE and optimal receivers, the sum spectral efficiency increases with the number of users, given a fixed total system load (summed over users). That is, the spectral efficiency is maximized when each user is assigned a single signature, and the number of users and processing gain both tend to infinity. In contrast, with isometric signatures other-user interference is worse than self-interference, so that the sum spectral efficiency decreases with the number of users. The comparison results with CDMA and OFDMA can be used to quantify the tradeoffs among spectral efficiency, receiver complexity, and versatility (e.g., the amount of user coordination) when providing a variable data rate service.

APPENDIX I MOMENTS OF \mathbf{R} AND $\underline{\mathbf{R}}$

Here we show that the first three (asymptotic) moments of $\underline{\mathbf{R}}$ and \mathbf{R} are identical, and that the difference in fourth moments is a polynomial in the set of loads $\{\alpha_j\}$ and powers $\{p_j\}$. We also show that the difference in the fourth moments is small compared with the magnitude of the fourth moments.

Let $P_j, j \in \mathcal{J}$, be a scalar random variable whose distribution is the a.e.d. of \mathbf{P}_j .

The incremental signature method⁹ is used to show the equality of the first three (asymptotic) moments of $\underline{\mathbf{R}}$ and \mathbf{R} , and that all terms in the polynomial for the difference in the fourth moment have the form $(\alpha_j \alpha_u)^2 \text{Var}[P_j] \text{Var}[P_u], j \neq u$, where $\text{Var}[P_j]$ denotes the variance of P_j . In general, the difference in the n th moments is a polynomial in the noise power σ_n^2 , the set of loads α_j , and the moments of $P_j, j \in \mathcal{J}$. In particular, the difference in the n th moments is a polynomial containing two types of terms. The first type has the same form as those found in the polynomial for the difference in the $(n-1)$ th moment, but multiplied by σ_n^2 . The second type has the form

$$c \prod_{j \in \mathcal{J}} \alpha_j^{a_j} \mathbf{E} [P_j^{m_{j,1}}]^{m_{j,2}} \quad (52)$$

where c is a constant (possibly zero), and for each $j \in \mathcal{J}$, $0 \leq a_j \leq n-2$, and $\sum_{j \in \mathcal{J}} a_j = n$. Also $m_{j,1}$, and $m_{j,2}$ are nonnegative integers with $m_{j,1} m_{j,2} = a_j$. Moreover, we find that for the moments computed here, a majority of significant terms in the moment polynomials cancel in the difference polynomials (e.g., terms such as $\text{Tr}[\mathbf{R}_j^n]$). Therefore, the difference in n th moments is small in comparison to the moment, especially for small α_j .

In principle, this comparison can be used to bound the approximation error incurred when replacing \mathbf{R} by $\underline{\mathbf{R}}$ in the expressions for optimal spectral efficiency and SINR for the MMSE receiver. We also remark that this moment analysis can be used to compute the *exact* SINR and spectral efficiency associated with a reduced-rank MMSE receiver [15], [30].

We require the following notation. Let $\boldsymbol{\alpha} = [\alpha_1, \dots, \alpha_J]^\dagger$. Also let

$$\nu_{n,N}(\boldsymbol{\alpha}) = \text{Tr}[\mathbf{R}^n] \quad (53)$$

$$\underline{\nu}_{n,N}(\boldsymbol{\alpha}) = \text{Tr}[\underline{\mathbf{R}}^n] \quad (54)$$

$$\underline{\nu}_{n,N}^\epsilon(\boldsymbol{\alpha}) = \underline{\nu}_{n,N}(\boldsymbol{\alpha}) - \nu_{n,N}(\boldsymbol{\alpha}) \quad (55)$$

$$\underline{\mathbf{P}}_j = \mathbf{U}_j^\dagger \mathbf{P}_j \mathbf{U}_j \quad (56)$$

We will require the following lemma for isometric signatures.

Lemma 1: Let \mathbf{S} be $K \leq N$ columns from an $N \times N$ Haar-distributed random matrix, and let \mathbf{s} be a column of \mathbf{S} . Let \mathbf{X}_N be an $N \times N$ random matrix with uniformly bounded spectral norm, which is a nontrivial function of \mathbf{S} , and satisfies $\mathbf{X}_N =$

⁹In [30, Appendix B], this incremental signature method was used for i.i.d. signatures and DS-CDMA. In this appendix, we extend the method to isometric signatures.

$\check{\mathbf{X}}_N$ where $\check{\mathbf{X}}_N$ is \mathbf{X} with \mathbf{S} substituted by $\mathbf{S}\mathbf{\Omega}$, and $\mathbf{\Omega}$ is an independent $K \times K$ unitary matrix. Then

$$\left| \mathbf{s}^\dagger \mathbf{X}_N \mathbf{s} - \frac{1}{\alpha N} \text{tr}[\mathbf{S}^\dagger \mathbf{X}_N \mathbf{S}] \right| \xrightarrow{\text{a.s.}} 0 \quad (57)$$

as $(N, K) \rightarrow \infty$ with $K/N \rightarrow \alpha$.

Proof: This is a straightforward extension of [13, Proposition 3]. \square

Additionally, using the definitions and assumptions of Lemma 1, note that if instead $\check{\mathbf{X}}_N$ is independent of \mathbf{S} , then

$$|\mathbf{s}^\dagger \mathbf{X}_N \mathbf{s} - \text{Tr}[\mathbf{X}_N]| \xrightarrow{\text{a.s.}} 0$$

under the limit given.

In what follows, we use the incremental signature technique with both i.i.d. and isometric signatures. For i.i.d. signatures, it is preferable to add a signature when deriving the derivative, whereas for isometric signatures we subtract a signature. This is because in the i.i.d. case, we can use [10, Lemma 1] when the incremental signature is independent of other terms in the expression. This occurs when the incremental signature is added. For isometric signatures, we can use Lemma 1 when the incremental signature is contained in \mathbf{R}_j . This occurs when the incremental signature is subtracted.

The following two lemmas are used to show convergence of random finite differences to deterministic derivatives for i.i.d. and isometric signatures, respectively.

Lemma 2: Let $\{\{a_{N,n}\}_{n=1 \dots \lfloor cN \rfloor}\}_{N=1, \dots}$ denote an infinite sequence, indexed by N , where the N th element is a complex-valued sequence, indexed by n , of length $\lfloor cN \rfloor$, $0 < c < \infty$. Suppose

$$\max_{n \leq \lfloor cN \rfloor} |N(a_{N,n+1} - a_{N,n}) - f'(n/N)| \xrightarrow{\text{a.s.}} 0 \quad (58)$$

as $N \rightarrow \infty$, where $f : [0, c] \mapsto \mathbb{R}$ is uniformly bounded above on $[0, c]$, and f' represents the derivative of f , which is assumed to be continuous. Additionally assume $|a_{N,0} - f(0)| \xrightarrow{\text{a.s.}} 0$ as $N \rightarrow \infty$. Then

$$|a_{N, \lfloor cN \rfloor} - f(c)| \xrightarrow{\text{a.s.}} 0 \quad (59)$$

as $N \rightarrow \infty$.

Proof:

$$|a_{N, \lfloor cN \rfloor} - f(c)| = \left| a_{N, \lfloor cN \rfloor} \pm \sum_{n=0}^{\lfloor cN \rfloor - 1} a_{N,n} - f(c) \right| \quad (60)$$

$$= \left| \sum_{n=0}^{\lfloor cN \rfloor - 1} (a_{N,n+1} - a_{N,n}) + a_{N,0} - f(c) \right| \quad (61)$$

$$= \left| \sum_{n=0}^{\lfloor cN \rfloor - 1} (a_{N,n+1} - a_{N,n}) + a_{N,0} \pm \frac{1}{N} \sum_{n=0}^{\lfloor cN \rfloor - 1} f'(n/N) - f(c) \right| \quad (62)$$

$$\leq \max_{n \leq \lfloor cN \rfloor} |N(a_{N,n+1} - a_{N,n}) - f'(n/N)| + |a_{N,0} - f(0)| + \left| f(0) + \frac{1}{N} \sum_{n=0}^{\lfloor cN \rfloor - 1} f'(n/N) - f(c) \right| \xrightarrow{\text{a.s.}} 0 \quad (63)$$

as $N \rightarrow \infty$, due to (58) and the Riemann integrability of f . Note that the symbol \pm is used as shorthand for $a \pm b \equiv a + b - b$. \square

Lemma 3: Let $\{\{a_{N,n}\}_{n=1 \dots \lfloor cN \rfloor}\}_{N=1, \dots}$ be as defined in Lemma 2, however with $0 < c \leq 1$. Suppose

$$\max_{\lfloor cN \rfloor \leq n \leq N} \left| N(a_{N,n} - a_{N,n-1}) - \left(\frac{m}{n/N} a_{N,n} + f(n/N) \right) \right| \xrightarrow{\text{a.s.}} 0 \quad (64)$$

as $N \rightarrow \infty$, where $f : [c, 1] \mapsto \mathbb{R}$ is continuous and uniformly bounded above on $[c, 1]$, and m is a finite positive integer. Additionally, assume $|a_{N,N} - C_0| \xrightarrow{\text{a.s.}} 0$ as $N \rightarrow \infty$, where $C_0 \in \mathbb{R}$ is a finite constant. Then

$$|a_{N, \lfloor cN \rfloor} - g(c)| \xrightarrow{\text{a.s.}} 0 \quad (65)$$

as $N \rightarrow \infty$, where $g(c) = c^m (C_0 - \int_c^1 f(x) x^{-m} dx)$.

Proof: Fix m . Note that the derivative of $g(c)$ is given by $g'(c) = \frac{m}{c} g(c) + f(c)$, and

$$\left| \left(g(1) - \frac{1}{N} \sum_{n=\lfloor cN \rfloor + 1}^N g'(n/N) \right) - g(c) \right| \rightarrow 0 \quad (66)$$

as $N \rightarrow \infty$. As such, define $g'_{N,n} = \frac{m}{n/N} a_{N,n} + f(n/N)$ for $\lfloor cN \rfloor \leq n \leq N$. Now

$$|a_{N, \lfloor cN \rfloor} - g(c)| = \left| a_{N, \lfloor cN \rfloor} \pm \sum_{n=\lfloor cN \rfloor + 1}^N a_{N,n} - g(c) \right| \quad (67)$$

$$= \left| a_{N,N} + \sum_{n=\lfloor cN \rfloor + 1}^N (a_{N,n-1} - a_{N,n}) - g(c) \right| \quad (68)$$

$$= \left| a_{N,N} + \sum_{n=\lfloor cN \rfloor + 1}^N (a_{N,n-1} - a_{N,n}) \pm \frac{1}{N} \sum_{n=\lfloor cN \rfloor + 1}^N g'_{N,n} - g(c) \right| \quad (69)$$

$$\leq \max_{\lfloor cN \rfloor + 1 \leq n \leq N} |N(a_{N,n} - a_{N,n-1}) - g'_{N,n}| + \left| g(1) - \frac{1}{N} \sum_{n=\lfloor cN \rfloor + 1}^N g'(n/N) - g(c) \right| + |a_{N,N} - C_0| + \frac{m}{c} \max_{\lfloor cN \rfloor + 1 \leq n \leq N} |a_{N,n} - g(n/N)| \xrightarrow{\text{a.s.}} 0 \quad (70)$$

as $N \rightarrow \infty$, due to (64) and (66). \square

We now address the difference in the asymptotic positive moments of \mathbf{R} and $\underline{\mathbf{R}}$. Clearly, the difference between the first moments is zero, i.e., $\nu_{1,N}^\epsilon(\boldsymbol{\alpha}) = 0$, since

$$\text{Tr}[\underline{\mathbf{R}}_j] = \text{Tr}[\mathbf{U}_j \mathbf{R}_j \mathbf{U}_j^\dagger] = \text{Tr}[\mathbf{R}_j].$$

The following Lemma is used to consider the difference in the second and third asymptotic moments of \mathbf{R} and $\underline{\mathbf{R}}$.

Lemma 4: For any $i, j, k \in \mathcal{J}$, we have (71)–(73) at the bottom of the page.

Proof: First note that $\text{Tr}[\underline{\mathbf{R}}_i^n] = \text{Tr}[\mathbf{R}_i^n]$ for integer $n \geq 0$, which establishes (71) when $i = j$. Now define $\varphi_{N, K_j} = \text{Tr}[\mathbf{R}_j^2]$. The incremental signature technique applied to φ_{N, K_j} involves the addition (subtraction) of an i.i.d. (isometric) signature \mathbf{s} to \mathbf{S}_j . This yields

$$N(\varphi_{N, K_j \pm 1} - \varphi_{N, K_j}) = \pm 2\mathbf{s}^\dagger \mathbf{H}_j^\dagger \mathbf{R}_j \mathbf{H}_j \mathbf{s} + (\mathbf{s}^\dagger \mathbf{P}_j \mathbf{s})^2 \quad (74)$$

Now, due to [10, Lemma 1] and Lemma 1, we have that

$$\mathbf{s}^\dagger \mathbf{H}_j^\dagger \mathbf{R}_j \mathbf{H}_j \mathbf{s} \xrightarrow{\text{a.s.}} \alpha_j \mathbf{E}[P_j^2]$$

and

$$|\mathbf{s}^\dagger \mathbf{H}_j^\dagger \mathbf{R}_j \mathbf{H}_j \mathbf{s} - \frac{1}{\alpha_j} \varphi_{N, K_j}| \xrightarrow{\text{a.s.}} 0$$

and similarly, $\mathbf{s}^\dagger \mathbf{P}_j \mathbf{s} \xrightarrow{\text{a.s.}} \mathbf{E}[P_j]$ for both signature types. In addition, note that $\varphi_{N, 0} = 0$ and $\varphi_{N, N} \xrightarrow{\text{a.s.}} \mathbf{E}[P_j^2]$ as $N \rightarrow \infty$ for i.i.d. and isometric signatures, respectively. Therefore, from Lemmas 2 and 3, we obtain the second and third lines of (73).

For the $i \neq j$ case in (73), it is convenient (for what follows) to evaluate the limit of

$$m_{N, K_{i(1)}, \dots, K_{i(L)}} = \text{Tr} \left[\prod_{\ell=1}^L \mathbf{R}_{i(\ell)} \right]$$

with $0 < L \leq J$, $i(\cdot) \in \mathcal{J}$, and $i(l) \neq i(m)$ for $l \neq m$ (i.e., distinct indices). Similarly, let

$$\underline{m}_{N, K_{i(1)}, \dots, K_{i(L)}} = \text{Tr} \left[\prod_{\ell=1}^L \underline{\mathbf{R}}_{i(\ell)} \right].$$

The incremental signature technique applied to $m_{N, K_{i(1)}, \dots, K_{i(L)}}$ and simplified via Lemmas 2 and 3 gives

$$|m_{N, K_{i(1)}, \dots, K_{i(L)}} - m(\boldsymbol{\alpha})| \xrightarrow{\text{a.s.}} 0$$

in the limit considered, where

$$\frac{\partial^L m(\boldsymbol{\alpha})}{\partial \alpha_{i(1)} \cdots \partial \alpha_{i(L)}} = \begin{cases} \prod_{\ell=1}^L \mathbf{E}[P_{i(\ell)}], & \text{i.i.d. sigs} \\ m(\boldsymbol{\alpha}) \prod_{\ell=1}^L \alpha_{i(\ell)}^{-1}, & \text{iso sigs} \end{cases} \quad (75)$$

with the boundary conditions $m(\boldsymbol{\alpha})$ is zero at $\boldsymbol{\alpha} = \mathbf{0}$ for i.i.d. \mathbf{S}_j , and

$$m(\boldsymbol{\alpha}) = \prod_{\ell=1}^L \mathbf{E}[P_{i(\ell)}]$$

at $\alpha_{i(\ell)} = 1 \ell = 1, \dots, L$ for isometric \mathbf{S}_j .

An identical treatment of $\underline{m}_{N, K_{i(1)}, \dots, K_{i(L)}}$ gives

$$|\underline{m}_{N, K_{i(1)}, \dots, K_{i(L)}} - \underline{m}(\boldsymbol{\alpha})| \xrightarrow{\text{a.s.}} 0$$

in the limit considered, where $\underline{m}_{N, K_{i(1)}, \dots, K_{i(L)}}$ and $\underline{m}(\boldsymbol{\alpha})$ satisfy the same relation given in (75) for $m_{N, K_{i(1)}, \dots, K_{i(L)}}$ and $m(\boldsymbol{\alpha})$, respectively. However, in order to obtain this it is also necessary to use the fact that in the limit considered

$$\left| \text{Tr} \left[\prod_{\ell=1}^L \underline{\mathbf{P}}_{i(\ell)} \right] - \prod_{\ell=1}^L \mathbf{E}[P_{i(\ell)}] \right| \xrightarrow{\text{a.s.}} 0 \quad (76)$$

for $i(\cdot) \in \mathcal{J}$, $i(l) \neq i(m)$ and $l \neq m$, due to the almost-sure asymptotic freeness of $\mathbf{P}_{i(\ell)}$, $\ell = 1, \dots, L$.

We therefore have the solution

$$m(\boldsymbol{\alpha}) = \underline{m}(\boldsymbol{\alpha}) = \prod_{\ell=1}^L \alpha_{i(\ell)} \mathbf{E}[P_{i(\ell)}]$$

establishing the $i \neq j$ case of (71), and also the first line of (73).

Now consider (72). Since $\text{tr}[\mathbf{A}\mathbf{B}] = \text{tr}[\mathbf{B}\mathbf{A}]$, we need only consider the cases $i = j = k$, $i = j \neq k$ and $i \neq j \neq k$. The $i = j = k$ case is readily obtained since $\text{Tr}[\underline{\mathbf{R}}_i^n] = \text{Tr}[\mathbf{R}_i^n]$ for integer $n \geq 0$. The $i \neq j \neq k$ case holds since $\underline{m}(\boldsymbol{\alpha}) = m(\boldsymbol{\alpha})$ (here $L = 3$). Finally, we consider $i = j \neq k$. Define $\vartheta_{N, K_i, K_k} = \text{Tr}[\mathbf{R}_i^2 \mathbf{R}_k]$, we have

$$\left| N(\vartheta_{N, K_i, K_k \pm 1} - \vartheta_{N, K_i, K_k}) - \begin{cases} v_{N, K_i, K_k}, & \text{i.i.d. sigs} \\ -\frac{1}{\alpha_k} \vartheta_{N, K_i, K_k}, & \text{iso sigs} \end{cases} \right| \xrightarrow{\text{a.s.}} 0 \quad (77)$$

in the limit considered, where $v_{N, K_i} = \text{Tr}[\mathbf{P}_k \mathbf{R}_i^2]$. In addition, note that $\vartheta_{N, K_i, 0} = 0$ and $\vartheta_{N, K_i, N} = v_{N, K_i}$ for i.i.d. and isometric signatures, respectively. In addition, we consider v_{N, K_i} in a similar manner to obtain (78) at the top of the following page in the limit considered, and note the boundary conditions $v_{N, 0} = 0$ and $|v_{N, N} - \mathbf{E}[P_k] \mathbf{E}[P_i^2]| \xrightarrow{\text{a.s.}} 0$ for i.i.d. and isometric signatures, respectively. Applying Lemmas 2 and 3 to (77) and (78), we obtain $v_{N, K_i} \xrightarrow{\text{a.s.}} v(\alpha_i)$ and $\vartheta_{N, K_i, K_k} \xrightarrow{\text{a.s.}} \vartheta(\boldsymbol{\alpha})$, where $v(\alpha_i)$ and $\vartheta(\boldsymbol{\alpha})$ are omitted, but may be obtained from the above. More significantly, the above derivations also hold for \mathbf{R}_i and \mathbf{R}_k replaced by $\underline{\mathbf{R}}_i$ and $\underline{\mathbf{R}}_k$, respectively, again due to (76), establishing (72). \square

$$|\text{Tr}[\mathbf{R}_i \mathbf{R}_j] - \text{Tr}[\underline{\mathbf{R}}_i \underline{\mathbf{R}}_j]| \xrightarrow{\text{a.s.}} 0 \quad (71)$$

$$|\text{Tr}[\mathbf{R}_i \mathbf{R}_j \mathbf{R}_k] - \text{Tr}[\underline{\mathbf{R}}_i \underline{\mathbf{R}}_j \underline{\mathbf{R}}_k]| \xrightarrow{\text{a.s.}} 0 \quad (72)$$

and

$$\text{Tr}[\mathbf{R}_i \mathbf{R}_j] \xrightarrow{\text{a.s.}} \begin{cases} \alpha_i \alpha_j \mathbf{E}[P_i] \mathbf{E}[P_j], & \text{for } i \neq j \\ \alpha_i^2 \mathbf{E}[P_i^2] + \alpha_i \mathbf{E}[P_i]^2, & \text{for } i = j \text{ and i.i.d. signatures} \\ \alpha_i^2 \text{Var}[P_i] + \alpha_i \mathbf{E}[P_i]^2, & \text{for } i = j \text{ and isometric signatures.} \end{cases} \quad (73)$$

$$\left| N(v_{N,K_i \pm 1} - v_{N,K_i}) - \begin{cases} 2\alpha_i \mathbf{E}[P_k] \mathbf{E}[P_i] + \mathbf{E}[P_k] \mathbf{E}[P_i]^2, & \text{i.i.d. sigs} \\ -\frac{2}{\alpha_i} v_{N,K_i} + \mathbf{E}[P_k] \mathbf{E}[P_i]^2, & \text{iso sigs} \end{cases} \right| \xrightarrow{\text{a.s.}} 0 \quad (78)$$

We now show that the differences in the second and third asymptotic moments of \mathbf{R} and $\underline{\mathbf{R}}$ are zero. From (73) of Lemma 4 we have

$$\begin{aligned} |\nu_{2,N}^\epsilon(\boldsymbol{\alpha})| &= |\text{Tr}[\underline{\mathbf{R}}^2] - \text{Tr}[\mathbf{R}^2]| \\ &\leq 2\sigma_n^2 \sum_{j \in \mathcal{J}} |\text{Tr}[\underline{\mathbf{R}}_j] - \text{Tr}[\mathbf{R}_j]| \\ &\quad + \sum_{j \in \mathcal{J}} \sum_{u \in \mathcal{J}} |\text{Tr}[\underline{\mathbf{R}}_j \underline{\mathbf{R}}_u] - \text{Tr}[\mathbf{R}_j \mathbf{R}_u]| \\ &\xrightarrow{\text{a.s.}} 0 \end{aligned} \quad (79)$$

and similarly, we can use (72) to show $|\nu_{3,N}^\epsilon(\boldsymbol{\alpha})| \xrightarrow{\text{a.s.}} 0$ in the limit considered.

Proceeding to the difference in the fourth moments of \mathbf{R} and $\underline{\mathbf{R}}$, we require the following lemma.

Lemma 5: For $i, j, k, l \in \mathcal{J}$

$$|\text{Tr}[\underline{\mathbf{R}}_i \underline{\mathbf{R}}_j \underline{\mathbf{R}}_k \underline{\mathbf{R}}_l] - \text{Tr}[\mathbf{R}_i \mathbf{R}_j \mathbf{R}_k \mathbf{R}_l]| \xrightarrow{\text{a.s.}} 0$$

in the limit considered unless

$$\{(i, j, k, l) | i = k, j = l, \text{ and } i \neq j\}.$$

Proof: As in the proof of Lemma 4, considering each case for (i, j, k, l) and applying the incremental signature technique gives the result. \square

From Lemmas 4 and 5 we have

$$\left| \nu_{4,N}^\epsilon(\boldsymbol{\alpha}) - \sum_{j \in \mathcal{J}} \sum_{k \in \mathcal{J}/\{j\}} (\phi_{N,K_j,K_k} - \phi_{N,K_j,K_k}) \right| \xrightarrow{\text{a.s.}} 0 \quad (80)$$

where

$$\phi_{N,K_j,K_k} = \text{Tr}[\underline{\mathbf{R}}_j \underline{\mathbf{R}}_k \underline{\mathbf{R}}_j \underline{\mathbf{R}}_k]$$

and

$$\phi_{N,K_j,K_k} = \text{Tr}[\mathbf{R}_j \mathbf{R}_k \mathbf{R}_j \mathbf{R}_k].$$

For i.i.d. signatures, the incremental signature technique and Lemma 2 gives $|\phi_{N,K_j,K_k} - \phi_{j,k}(\boldsymbol{\alpha})| \xrightarrow{\text{a.s.}} 0$, where

$$\frac{\partial}{\partial \alpha_j} \phi_{jk}(\boldsymbol{\alpha}) = 2\omega_{jk}(\boldsymbol{\alpha}) + \mathbf{E}[P_k]^2 \mathbf{E}[P_j]^2 \alpha_k^2 \quad (81)$$

$$\frac{\partial}{\partial \alpha_k} \omega_{jk}(\boldsymbol{\alpha}) = \psi_{jk}(\boldsymbol{\alpha}) + \psi_{kj}(\boldsymbol{\alpha}) + \mathbf{E}[P_k]^2 \mathbf{E}[P_j]^2 \alpha_j \quad (82)$$

$$\frac{\partial}{\partial \alpha_k} \psi_{jk}(\boldsymbol{\alpha}) = \alpha_j \lim \text{Tr}[\mathbf{P}_j \mathbf{P}_k \mathbf{P}_j \mathbf{P}_k]. \quad (83)$$

Integrating gives

$$\begin{aligned} \phi_{jk}(\boldsymbol{\alpha}) &= \alpha_j^2 \alpha_k^2 \lim \text{Tr}[\mathbf{P}_j \mathbf{P}_k \mathbf{P}_j \mathbf{P}_k] \\ &\quad + \mathbf{E}[P_k]^2 \mathbf{E}[P_j]^2 (\alpha_j^2 \alpha_k + \alpha_k^2 \alpha_j). \end{aligned} \quad (84)$$

The same technique applied to ϕ_{N,K_j,K_k} gives an expression identical to (84), but where $\text{Tr}[\mathbf{P}_j \mathbf{P}_k \mathbf{P}_j \mathbf{P}_k]$ is replaced by $\text{Tr}[\underline{\mathbf{P}}_j \underline{\mathbf{P}}_k \underline{\mathbf{P}}_j \underline{\mathbf{P}}_k]$. Note that

$$\text{Tr}[\mathbf{P}_j \mathbf{P}_k \mathbf{P}_j \mathbf{P}_k] \xrightarrow{\text{a.s.}} \mathbf{E}[P_j^2] \mathbf{E}[P_k^2] \quad (85)$$

$$\begin{aligned} \text{Tr}[\underline{\mathbf{P}}_j \underline{\mathbf{P}}_k \underline{\mathbf{P}}_j \underline{\mathbf{P}}_k] &\xrightarrow{\text{a.s.}} \mathbf{E}[P_j]^2 \mathbf{E}[P_k]^2 \\ &\quad + \mathbf{E}[P_k]^2 \mathbf{E}[P_j^2] - \mathbf{E}[P_j]^2 \mathbf{E}[P_k]^2 \end{aligned} \quad (86)$$

where (86) is found by applying the method for calculating mixed moments of free random variables (e.g., see [31]). For i.i.d. signatures we combine (80), (84), and (85)–(86) to obtain

$$\left| \nu_{4,N}^\epsilon(\boldsymbol{\alpha}) + \sum_{j \in \mathcal{J}} \sum_{k \in \mathcal{J}/\{j\}} \text{Var}[P_j] \text{Var}[P_k] (\alpha_j \alpha_k)^2 \right| \xrightarrow{\text{a.s.}} 0. \quad (87)$$

For isometric signatures we also have

$$|\phi_{N,K_j,K_k} - \phi_{j,k}(\boldsymbol{\alpha})| \xrightarrow{\text{a.s.}} 0$$

from the incremental signature technique and Lemma 3, where

$$\phi_{jk}(\boldsymbol{\alpha}) = \alpha_j^2 \varpi_{jk}(\alpha_k) + \alpha_j (1 - \alpha_j) (\alpha_k \mathbf{E}[P_j] \mathbf{E}[P_k])^2 \quad (88)$$

$$\varpi_{jk}(\alpha_k) = C_2 \alpha_k^2 + (\mathbf{E}[P_j] \mathbf{E}[P_k])^2 \alpha_k \quad (89)$$

$$C_2 = \lim \text{Tr}[\mathbf{P}_j \mathbf{P}_k \mathbf{P}_j \mathbf{P}_k] - (\mathbf{E}[P_j] \mathbf{E}[P_k])^2. \quad (90)$$

The same technique applied to ϕ_{N,K_j,K_k} also gives (88)–(90) where $\text{Tr}[\mathbf{P}_j \mathbf{P}_k \mathbf{P}_j \mathbf{P}_k]$ is replaced by $\text{Tr}[\underline{\mathbf{P}}_j \underline{\mathbf{P}}_k \underline{\mathbf{P}}_j \underline{\mathbf{P}}_k]$, given by (86). Thus, for isometric signatures we again combine (80) and (88), so that $\nu_{4,N}^\epsilon(\boldsymbol{\alpha})$ with isometric signatures also satisfies (87).

Finally, observe that the limit of $\nu_{4,N}^\epsilon(\boldsymbol{\alpha})$ is a polynomial in the per-user system loads α_j and the variance of the subchannel powers, $\text{Var}[P_j]$, $j \in \mathcal{J}$. Fig. 1, presented earlier, showed that for $n = 4$ the numerical value of (87) is small in comparison to the moment $\nu_{4,N}(\boldsymbol{\alpha})$ over the wide range of $\boldsymbol{\alpha}$ and the two values of SNR shown. This is largely due to the fact that only $J(J-1)$ terms are nonzero out of the total $(J+1)^4$ terms in the expansion of (80).

By extension, we see that the limit of $\nu_{n,N}^\epsilon(\boldsymbol{\alpha})$ is a polynomial in the loads α_j , and the moments of P_j , as shown in (52). For $n > 4$, the noise power σ_n^2 enters terms with degree $n-4$ as well.¹⁰

APPENDIX II

ALMOST-SURE LIMIT DISTRIBUTION OF \mathbf{R}

Proof of Theorem 1: The proof is by induction on I . Note that the family \mathcal{S}_J^0 has an almost-sure limit distribution, since for any $\underline{m} \in \mathcal{M}(I+J+1)$, $\kappa_{\underline{m},N}$ in (17) clearly has an almost-sure

¹⁰The noise power does not appear in the moment difference for $n \leq 4$ since it only appears in $\nu_{n,N}^\epsilon(\boldsymbol{\alpha})$ as a coefficient of terms which are asymptotically identical for both \mathbf{R} and $\underline{\mathbf{R}}$, e.g., $\sigma_n^2 \text{Tr}[\mathbf{R}_i^3]$

limit of the form $\sigma_n^{2a_0} \mathbf{E}[P_1^{a_1}] \cdots \mathbf{E}[P_J^{a_J}]$ for some integers $0 \leq a_j < \infty$ and $j = 0, \dots, J$. Observe this limit is a polynomial of degree $d_{\underline{m},j} = 0$ in α_j , $j = 1, \dots, J$.

Now assume the family \mathcal{S}_J^{I-1} has an almost-sure limit distribution for some $0 < I < J$, and hence, $\kappa_{\underline{m},N} \xrightarrow{\text{a.s.}} \kappa_{\underline{m}}$ in the limit considered for all $\underline{m} \in \mathcal{M}(I+J)$ where $\kappa_{\underline{m}}$ is a polynomial of degree $d_{\underline{m},j}$ in α_j for all $j = 1, \dots, I-1$ with coefficients determined by σ_n^2 and finite moments of P_j , $j = 1 \dots J$ (hereafter, refer to this as $\kappa_{\underline{m}}$ having “the stated form”). For the induction argument on I , we wish to show that \mathcal{S}_J^I has an almost-sure limit distribution, and that for all $\underline{m} \in \mathcal{M}(I+J+1)$, $\kappa_{\underline{m},N} \xrightarrow{\text{a.s.}} \kappa_{\underline{m}}$ in the limit considered, where $\kappa_{\underline{m}}$ has the stated form.

To do this, we use a further induction argument on $d_{\underline{m},j}$. We start this induction by noting that due to the previous inductive assumption, for all $\underline{m} \in \mathcal{M}(I+J+1)$ with $d_{\underline{m},I} = 0$, $\kappa_{\underline{m},N} \xrightarrow{\text{a.s.}} \kappa_{\underline{m}}$ in the limit considered, where $\kappa_{\underline{m}}$ has the stated form, since the trace in (17) contains only \mathbf{R}_j for $j < I$. Therefore, for this induction argument, assume that for all $\underline{m} \in \mathcal{M}(I+J+1)$ with $d_{\underline{m},I} < D$, where D is a finite positive integer, $\kappa_{\underline{m},N} \xrightarrow{\text{a.s.}} \kappa_{\underline{m}}$ in the limit considered, where $\kappa_{\underline{m}}$ has the stated form.

We now demonstrate that for all $\underline{m} \in \mathcal{M}(I+J+1)$ with $d_{\underline{m},I} = D$, $\kappa_{\underline{m},N} \xrightarrow{\text{a.s.}} \kappa_{\underline{m}}$ in the limit considered, where $\kappa_{\underline{m}}$ has the stated form. To do this, we use the incremental-signature technique with respect to user I . To do this, we consider a sequence \underline{m} for which $d_{\underline{m},I} = D$, and indicate the dependence of $\kappa_{\underline{m},N}$ and $\kappa_{\underline{m}}$ on K_I and α_I by writing $\kappa_{\underline{m},N} \equiv \kappa_{\underline{m},N,K_I}$ and $\kappa_{\underline{m}} \equiv \kappa_{\underline{m}}(\alpha_I)$.

We have

$$\kappa_{\underline{m},N,K_I \pm 1} = \text{Tr} \left[\prod_{i=1}^{|\underline{m}|} \left(\mathbf{X}_{\underline{m}(i)} \pm \delta_{I,\underline{m}(i)} \mathbf{H}_I \mathbf{s} \mathbf{s}^\dagger \mathbf{H}_I^\dagger \right) \right] \quad (91)$$

where $\delta_{a,b}$ is unity when $a = b$ and zero otherwise, and the \pm sign in (91) and in what follows is positive for i.i.d. signatures and negative for isometric signatures, as discussed in Appendix I. Note that (91) holds for general sequences \underline{m} ; however, in this induction step we will only be concerned with sequences for which $d_{\underline{m},I} = D > 0$.

Expanding (91) gives

$$N(\kappa_{\underline{m},N,K_I \pm 1} - \kappa_{\underline{m},N,K_I}) = \sum_{b=1}^{2^{|\underline{m}|-1}} T(b) \quad (92)$$

$$T(b) = \text{tr} \left[\prod_{i=1}^{|\underline{m}|} \tau_{b,i} \right] \quad (93)$$

$$\tau_{b,i} = \begin{cases} \mathbf{X}_{\underline{m}(i)}, & \text{if the } i\text{th bit of } b \text{ is zero} \\ \pm \delta_{I,\underline{m}(i)} \mathbf{H}_I \mathbf{s} \mathbf{s}^\dagger \mathbf{H}_I^\dagger & \text{otherwise} \end{cases} \quad (94)$$

where the i th bit of b refers to the standard binary representation of the $|\underline{m}|$ -bit positive integer b , defining the most significant bit as the “first” bit.

Suppose there are $n_I(b)$ terms of the form $\mathbf{H}_I \mathbf{s} \mathbf{s}^\dagger \mathbf{H}_I^\dagger$ in the product in (93). Note that there will always be at least one term of this form, since $D > 0$ and $b \neq 0$. So $1 \leq n_I(b) \leq m$. Also, from the expansion of (91), the degree of \mathbf{R}_I in $T(b)$ is equal to $D - n_I(b)$, and is therefore at most $D - 1$.

In other words, the argument of the trace in $T(b)$ is a product of $|\underline{m}|$ terms, given in (94), where there are precisely $n_I(b) > 0$ which have the form $\mathbf{H}_I \mathbf{s} \mathbf{s}^\dagger \mathbf{H}_I^\dagger$. We now use the fact that $\text{tr}[\mathbf{AB}] = \text{tr}[\mathbf{BA}]$ to create products of terms in which $\mathbf{s}^\dagger \mathbf{H}_I^\dagger$ appears on the left and $\mathbf{H}_I \mathbf{s}$ appears on the right.

More precisely, we now have

$$T(b) = \pm \prod_{\ell=1}^{n_I(b)} t_{b,\ell} \quad (95)$$

$$t_{b,\ell} = \mathbf{s}^\dagger \mathbf{H}_I^\dagger \left(\delta_{0,m_{b,\ell}} \mathbf{I} + \prod_{\epsilon=0}^{m_{b,\ell}-1} \mathbf{X}_{\underline{m}(s_{b,\ell} \oplus \epsilon)} \right) \mathbf{H}_I \mathbf{s} \quad (96)$$

where $0 \leq m_{b,\ell} < |\underline{m}|$ denotes the number of terms between the ℓ th $(\mathbf{s}^\dagger \mathbf{H}_I^\dagger, \mathbf{H}_I \mathbf{s})$ pair in $T(b)$, and \oplus denotes modulo- $|\underline{m}|$ addition. Also, $1 \leq s_{b,\ell} \leq |\underline{m}|$ denotes the bit index at which the first term of the form \mathbf{X}_{i_k} occurs between the ℓ th $(\mathbf{s}^\dagger \mathbf{H}_I^\dagger, \mathbf{H}_I \mathbf{s})$ pair in $T(b)$. Now applying [10, Lemma 1] and Lemma 1 to (96), we have that $|t_{b,\ell} - \hat{t}_{b,\ell}| \xrightarrow{\text{a.s.}} 0$ in the limit considered, where we get (97) at the bottom of the page due to [10, Lemma 1] in the i.i.d. case and Lemma 1 in the isometric case.

Consider sequences \underline{m} of interest, i.e., those for which $d_{\underline{m},I} = D$. For i.i.d. signatures it is apparent that the product term in the right-hand side of (97) is a monomial in elements of \mathcal{S}_J^I having degree with respect to \mathbf{R}_I less than D . This is due to the fact that $\hat{t}_{b,\ell}$ has at most the same degree as $T(b)$, which we previously established is at most $D - 1$. Similarly, for isometric signatures it is apparent that the right-hand side of (97) is either equal to $\frac{1}{\alpha_I} \kappa_{\underline{m},N,K_I}$ (this occurs D times, corresponding to when $n_I(b) = 1$), or has a trace argument which is a monomial in variables from \mathcal{S}_J^I having degree with respect to \mathbf{R}_I less than D .

For i.i.d. signatures, and isometric signatures for the cases where $\hat{t}_{b,\ell}$ does not equal $\frac{1}{\alpha_I} \kappa_{\underline{m},N,K_I}$, according to the induction assumptions we have now established that $\hat{t}_{b,\ell}$ almost-surely converges to a polynomial in α_j with degree equal to the degree of \mathbf{R}_j in the argument of the trace in (97) for $j = 1, \dots, I$, and coefficients determined by σ_n^2 and moments of P_j , $j = 1, \dots, J$. Moreover, for these cases, $T(b)$ almost-surely converges to a deterministic polynomial in α_j , $j = 1, \dots, I - 1$, of at most degree $d_{\underline{m},j}$, and in α_I with degree at most $D - 1$ for i.i.d. signatures, and with degree $D - 2$ for isometric signatures.

$$\hat{t}_{b,\ell} = \begin{cases} \mathbf{E}[P_I], & m_{b,\ell} = 0, \\ \text{Tr} \left[\mathbf{P}_I \prod_{\epsilon=0}^{m_{b,\ell}-1} \mathbf{X}_{\underline{m}(s_{b,\ell} \oplus \epsilon)} \right], & m_{b,\ell} \neq 0, \text{ i.i.d. sigs} \\ \frac{1}{\alpha_I} \text{Tr} \left[\mathbf{R}_I \prod_{\epsilon=0}^{m_{b,\ell}-1} \mathbf{X}_{\underline{m}(s_{b,\ell} \oplus \epsilon)} \right], & m_{b,\ell} \neq 0, \text{ iso sigs.} \end{cases} \quad (97)$$

Therefore, for any sequence $\{i_k\}_{k=1,\dots,m}$ for which $d_{\underline{m},I} = D \geq 0$, we can write (92) in the following general form:

$$\left| N(\kappa_{\underline{m},N,K_I+1} - \kappa_{\underline{m},N,K_I}) - \sum_{\ell=0}^{D-1} c_{\ell}^{\text{i.i.d.}} \alpha_I^{\ell} \right| \xrightarrow{\text{a.s.}} 0, \quad \text{i.i.d. sigs} \quad (98)$$

$$\left| N(\kappa_{\underline{m},N,K_I} - \kappa_{\underline{m},N,K_I-1}) - \left(\frac{D}{\alpha_I} \kappa_{\underline{m},N,K_I} + \sum_{\ell=0}^{D-2} c_{\ell}^{\text{iso}} \alpha_I^{\ell} \right) \right| \xrightarrow{\text{a.s.}} 0, \quad \text{iso sigs} \quad (99)$$

where $c_{\ell}^{\text{i.i.d.}}, \ell = 0, \dots, D-1$ and $c_{\ell}^{\text{iso}}, \ell = 0, \dots, D-2$ are deterministic values which do not depend on α_I . In addition, considering the boundary conditions, note that we also have from the inductive assumption that $\kappa_{\underline{m},N,0}$ and $\kappa_{\underline{m},N,N}$ for i.i.d. and isometric signatures, respectively, almost-surely converge to deterministic polynomials in $\alpha_j, j = 1, \dots, I-1$, of at most degree $d_{\underline{m},j}$. And so, we may apply Lemmas 2 and 3 to obtain that $\kappa_{\underline{m},N,K_I} \xrightarrow{\text{a.s.}} \kappa_{\underline{m}}(\alpha_I)$, where $\kappa_{\underline{m}}(\alpha_I)$ is a polynomial of degree D in α_I , given by

$$\kappa_{\underline{m}}(\alpha_I) = \sum_{\ell=1}^D \frac{c_{\ell-1}^{\text{i.i.d.}}}{\ell} \alpha_I^{\ell}, \quad \text{i.i.d. signatures} \quad (100)$$

$$\kappa_{\underline{m}}(\alpha_I) = c_D^{\text{iso}} \alpha_I^D + \sum_{\ell=1}^{D-1} \frac{c_{\ell-1}^{\text{iso}}}{\ell - D} \alpha_I^{\ell}, \quad \text{isometric signatures} \quad (101)$$

where

$$c_D^{\text{iso}} = c - \sum_{\ell=1}^{D-1} \frac{c_{\ell-1}^{\text{iso}}}{\ell - D}$$

and c is the boundary condition found via $|\kappa_{\underline{m},N,N} - c| \xrightarrow{\text{a.s.}} 0$.

Moreover, this completes the induction and implies that \mathcal{S}_I^J has an almost-sure limit distribution. \square

Under the assumption of a positive compact distribution for $P_j, j \in \mathcal{J}$, and the well-known fact that $\|\mathcal{S}_j \mathcal{S}_j^{\dagger}\| < (1 + \sqrt{\alpha_j})^2$, Theorem 1 implies the almost-sure convergence in distribution of the empirical distribution function of \mathbf{R} to a deterministic distribution with compact support.

ACKNOWLEDGMENT

The authors thank Ralf R. Müller for several helpful discussions, and specifically, for providing an example showing that the matrices being summed in \mathbf{R} are not asymptotically free.

REFERENCES

- [1] J. Chen and U. Mitra, "Optimum near-far resistance for dual-rate DS/CDMA signals: Random signature sequence analysis," *IEEE Trans. Inf. Theory*, vol. 45, no. 7, pp. 2434–2447, Nov. 1999.
- [2] S. Ulukus, E. Biglieri, and M. Z. Win, "Optimum modulation and multicode formats in CDMA systems with multiuser receivers," *Proc. IEEE INFOCOM 2001*, vol. 1, pp. 395–402, Apr. 2001.
- [3] Y. Yao, H. V. Poor, and F. W. Sun, "User capacity for synchronous multirate CDMA systems with linear MMSE receivers," *IEEE Trans. Inf. Theory*, vol. 50, no. 11, pp. 2785–2793, Nov. 2004.
- [4] N. Yee, J. P. Linnartz, and G. Fettweis, "Multi-carrier CDMA in indoor wireless radio networks," in *Proc. PIMRC'93*, Yokohama, Japan, Sep. 1993, pp. 109–113.
- [5] P. M. Crespó, M. L. Honig, and J. A. Salehi, "Spread-time code-division multiple access," *IEEE Trans. Commun.*, vol. 43, no. 6, pp. 2139–2148, Jun. 1995.
- [6] S. Verdú and S. Shamai (Shitz), "Spectral efficiency of CDMA with random spreading," *IEEE Trans. Inf. Theory*, vol. 45, no. 2, pp. 622–640, Mar. 1999.
- [7] S. Shamai (Shitz) and S. Verdú, "The impact of frequency-flat fading on the spectral efficiency of CDMA," *IEEE Trans. Inf. Theory*, vol. 47, no. 4, pp. 1302–1327, May 2001.
- [8] A. J. Grant and P. D. Alexander, "Random sequence multisets for synchronous code-division multiple-access channels," *IEEE Trans. Inf. Theory*, vol. 44, no. 7, pp. 2832–2836, Nov. 1998.
- [9] D. N. C. Tse and S. V. Hanly, "Linear multiuser receivers: Effective interference, effective bandwidth and user capacity," *IEEE Trans. Inf. Theory*, vol. 45, no. 2, pp. 641–657, Mar. 1999.
- [10] J. Evans and D. N. C. Tse, "Large system performance of linear multiuser receivers in multipath fading channels," *IEEE Trans. Inf. Theory*, vol. 46, no. 6, pp. 2059–2078, Sep. 2000.
- [11] W. G. Phoel and M. L. Honig, "Performance of coded DS-SS with pilot-assisted channel estimation and linear interference suppression," *IEEE Trans. Commun.*, vol. 50, no. 5, pp. 822–832, May 2002.
- [12] E. Biglieri, G. Caire, and G. Taricco, "CDMA system design through asymptotic analysis," *IEEE Trans. Commun.*, vol. 48, no. 7, pp. 1882–1896, Nov. 2000.
- [13] M. Debbah, W. Hachem, P. Loubaton, and M. de Courville, "MMSE analysis of certain large isometric random precoded systems," *IEEE Trans. Inf. Theory*, vol. 49, no. 5, pp. 1293–1311, May 2003.
- [14] M. J. M. Peacock, I. B. Collings, and M. L. Honig, "Asymptotic analysis of MMSE multiuser receivers for multi-signature multicarrier CDMA in Rayleigh fading," *IEEE Trans. Commun.*, vol. 52, no. 6, pp. 964–972, Jun. 2004.
- [15] L. Li, A. M. Tulino, and S. Verdú, "Design of reduced-rank MMSE multiuser detectors using random matrix methods," *IEEE Trans. Inf. Theory*, vol. 50, no. 6, pp. 986–1008, Jun. 2004.
- [16] D. Voiculescu, *Free Probability Theory (Fields Institute Communications)*. Providence, RI: Amer. Math. Soc., 1997, vol. 12.
- [17] F. Hiai and D. Petz, *The Semicircle Law, Free Random Variables and Entropy*. Providence, RI: Amer. Math. Soc., 2000, vol. 77, Mathematical Surveys and Monographs.
- [18] R. R. Müller, "A random matrix model of communication via antenna arrays," *IEEE Trans. Inf. Theory*, vol. 48, no. 9, pp. 2495–2506, Sep. 2002.
- [19] E. Biglieri, G. Taricco, and A. Tulino, "Performance of space-time codes for a large number of antennas," *IEEE Trans. Inf. Theory*, vol. 48, no. 7, pp. 1794–1803, Jul. 2002.
- [20] A. M. Tulino and S. Verdú, "Random matrix theory and wireless communications," *Found. and Trends in Commun. and Inf. Theory*, vol. 1, no. 1, pp. 1–182, 2004.
- [21] S. Verdú, "Capacity region of Gaussian CDMA channels: The symbol-synchronous case," in *Proc. 24th Allerton Conf. Communication, Control and Computing*, Monticello, IL, Oct. 1986, pp. 1025–1034.
- [22] M. J. M. Peacock, I. B. Collings, and M. L. Honig, "Eigenvalue distributions of sums and products of large random matrices via incremental matrix expansions," *IEEE Trans. Inf. Theory*, submitted for publication.
- [23] J. W. Silverstein and Z. D. Bai, "On the empirical distribution of eigenvalues of a class of large dimensional random matrices," *J. Multivar. Anal.*, vol. 54, no. 2, pp. 175–192, 1995.
- [24] V. L. Girko, *Theory of stochastic Canonical Equations*. Norwell, MA: Kluwer Academic, 2001.
- [25] D. Voiculescu, "Multiplication of certain noncommuting random variables," *J. Oper. Theory*, vol. 18, pp. 223–235, 1987.
- [26] D. Guo, S. Verdú, and L. K. Rasmussen, "Asymptotic normality of linear multiuser receiver outputs," *IEEE Trans. Inf. Theory*, vol. 48, no. 12, pp. 3080–3095, Dec. 2002.
- [27] T. Cover and J. Thomas, *Elements of Information Theory*. New York: Wiley, 1991.
- [28] J. W. Silverstein, "Strong convergence of the empirical distribution of eigenvalues of large dimensional random matrices," *J. Multivar. Anal.*, vol. 55, no. 2, pp. 331–339, 1995.
- [29] V. V. Veeravalli and A. Mantravadi, "The coding-spreading tradeoff in CDMA systems," *IEEE J. Sel. Areas Commun.*, vol. 20, no. 2, pp. 396–408, Feb. 2002.
- [30] M. L. Honig and W. Xiao, "Performance of reduced-rank linear interference suppression," *IEEE Trans. Inf. Theory*, vol. 47, no. 5, pp. 1928–1946, Jul. 2001.
- [31] P. Biane, "Free probability for probabilists," unpublished manuscript, 2000.
- [32] K. L. Chung, *A Course in Probability Theory*, 3rd ed. San Diego, CA: Academic, 2001.
- [33] M. J. M. Peacock, I. B. Collings, and M. L. Honig, "Asymptotic spectral efficiency regions of two-user MC-CDMA systems in frequency-selective Rayleigh fading," in *Proc. IEEE Conf. Communication (ICC)*, vol. 2, Paris, France, Jun. 2004, pp. 957–961.